INVESTIGATION OF THE MECHANICAL BEHAVIOR OF SEVERELY DEFORMED ALUMINUM ALLOY UNDER MULTI-DIRECTIONAL FORGING

A Thesis

by

Burak Bahat

Submitted to the
Graduate School of Sciences and Engineering
In Partial Fulfillment of the Requirements for
the Degree of

Master of Science

in the
Department of Mechanical Engineering

Özyeğin University
March 2023

INVESTIGATION OF THE MECHANICAL BEHAVIOR OF SEVERELY DEFORMED ALUMINUM ALLOY UNDER MULTI-DIRECTIONAL FORGING

Approved by:

Prof. Dr. Güney Güven Yapıcı, Advisor
Department of Mechanical Engineering
Head of Department
Özyeğin University

Asst. Prof. Dr. Altuğ Melik Başol
Department of Mechanical Engineering
Özyeğin University

Asst. Prof. Dr. Mehmet İpekoğlu
Department of Mechanical Engineering
Turkish-German University

Date Approved: 27 March 2023

To My Wife & Son, Family, and Friends . . .

ABSTRACT

Aluminum alloys are widely used for lightweight applications. Severe plastic deformation has recently emerged as a versatile method to deliver large strains and thereby improve mechanical properties. Among these methods, it is seen that the versatile forging (MAF) process stands out in terms of its industrial applicability. In particular, it has been determined that the strength of some metals is significantly increased by the warm or hot forging process. In this study, the mechanical properties of Al 6061 alloy, which is frequently used in the automotive and aviation industries, were improved by the multi-axial forging method and its behavior was characterized. For this, 3, 6, 9 and 12 pass forging processes were carried out at 200 °C temperature by designing an experiment. The Split Hopkinson Pressure Bar assembly was designed and built to analyze the mechanical behavior after application.

As a result of the tests, it was determined that the yield, tensile and hardness values of the Al alloys forged with the multiaxial forging method increased up to a certain cycle, and the grain structures were reduced in the microstructure examinations. In the aluminum 6xxx alloys used in this study, because of 6 passes forging, the hardness value was 80 HB, yield strength was 245 MPa, and tensile strength was 270 MPa, while the average grain size was 8.32µm. As a result of 9 passes of forging of the same alloy, the hardness, yield, and tensile values decreased compared to 6 passes of forging, while the grain size increased, the values are 73HB, 212 MPa, 232 MPa and 11.54µm, respectively. Similar results were obtained in the SHPB test, which is a dynamic crash test, and it was determined that the mechanical properties of the Aluminum 6xxx series alloys were improved by the multi-axial forging method.

ÖZETÇE

Alüminyum alaşımları, hafif uygulamalar için yaygın olarak kullanılmaktadır. Şiddetli plastik deformasyon, son zamanlarda büyük gerinimler vermek ve böylece mekanik özellikleri geliştirmek için çok yönlü bir yöntem olarak ortaya çıkmıştır. Bu yöntemler arasında endüstriyel uygulanabilirliği açısından çok yönlü / eksenli dövme (MDF / MAF) işleminin ön plana çıktığı görülmektedir. Özellikle bazı metallerin ılık veya sıcak dövme işlemi ile mukavemetlerinin önemli oranda artırıldığı belirlenmiştir.

Bu çalışmada otomotiv ve havacılık sektöründe çok sık kullanılan Al 6061 alaşımının mekanik özellikleri çok eksenli dövme yöntemi ile iyileştirilerek davranışı karakterize edilmiştir. Bunun için deney tasarımı yapılarak 200 °C sıcaklıkta 3, 6, 9 ve 12 paso dövme işlemleri gerçekleştirilmiştir. Uygulama sonrası mekanik davranışı analiz etmek için Split Hopkinson Basınçlı Bar düzeneği tasarlanarak inşa edilmiştir.

Yapılan testler sonucu çok eksenli dövme yöntemi ile dövülen Al alaşımlarının belli bir çevrime kadar akma, çekme ve sertlik değerlerinin arttığı bununla beraber mikroyapı incelemelerinde tane yapılarının küçüldüğü tespit edilmiştir. Bu çalışmada kullanılan alüminyum 6061 alaşımında 6 paso dövme işlemi sonucu sertlik değeri 80 HB, akma mukavemeti 245 MPa ve çekme mukavemeti 270 MPa iken ortalama tane boyutu 8.32µm elde edilmiştir. Aynı alaşımın 9 paso dövülmesi sonucu sertlik, akma ve çekme değeri 6 paso dövmeye göre düşerken tane boyutu ise büyümüştür, değerler sırasıyla 73HB, 212 MPa, 232 MPa ve 11.54µm şeklindedir. Benzer sonuçlar dinamik çarpışma testi olan SHPB testinde de alınarak Alüminyum 6xxx serisi alaşımları için çok eksenli dövme yöntemi ile mekanik özelliklerinin iyileştiği tespit edilmiştir.

ACKNOWLEDGEMENTS

To begin, I would want to express my profound appreciation to my family for the unending love and assistance that they have provided me throughout my life.

In addition, I would like to extend my sincerest gratitude to my supervisor, Professor Dr. Güney Güven Yapıcı, for the assistance and direction he has provided me with. I am indebted to him for the consistent support and help he has provided during the course of the present investigation, and I thank him for both of those things. In addition, I would like to express my gratitude to Mr. Ulaş Yıldırım, the technician who works in our manufacturing laboratory, for the efforts that he made to this study, as well as to the other members of my MEMFIS group. I would like to express my gratitude, in particular, to Eng. Amin Radi for the helpful advice and recommendations he provided. Special thanks to the managers and engineers of the BIRINCI R&D center for their valuable support and contributions during MDF trials.

TABLE OF CONTENTS

LIST OF TABLES

LIST OF FIGURES

CHAPTER I

INTRODUCTION

1.1 Motivation

The average grain size of the material typically plays a crucial and prevailing role in determining the mechanical and physical properties of all crystalline materials. Severe plastic deformation (SPD) is a well-known method for altering the grain size and shape of many different types of materials. ECAP (Equal Channel Angular Pressing), ARB (Accumulative Roll Bonding), HPT (High Pressure Torsion), and MAF/MAC (Multi Axial Forging/Compression), sometimes known as Multi-Directional Forging, have all been used to accomplish SPD. From a practical standpoint, it is generally acknowledged that applying SPD to bulk billets seems to be the most promising processing method for producing Al alloys with nanostructures [1-7].

Since they have such excellent chemical, physical, mechanical, and processing properties as low density, acceptable strength, good ductility, excellent oxidation resistance both at room temperature and above, and good formability, aluminum alloys like Al-6061 are currently the most widely used materials in almost all industries. Al-6061 alloys are typically utilized to create high-performance products with precise microstructures because they can survive significant deformation at high temperatures. Aluminum alloys are used in the aerospace and aviation industries because they are substantially lighter than steel and because every kilogram of weight loss leads to greater fuel savings and increased payload. With petrol prices rising and the necessity to lighten vehicles becoming more and more important, the automotive industry has increased its usage of aluminum over time. Aluminum is used mostly to lighten products today, but it has always been widely used since it is simple to mill, cast, extrude, roll, etc., and many alloys may be age-hardened (like 6061) [8-12]. Samples of Al6061 that had undergone multi-axial forging also displayed good ductility and strength. A uniform microstructure with an ultrafine grain shape was produced by processing this alloy using MAF at specific temperatures [13].

1.2 Research Objectives

The study's primary goal is to investigate the alterations in microstructure and mechanical properties of Al 6061 series Aluminum alloy by multiaxial forging plastic deformation method, and the results obtained in SEM, tensile test, hardness test, and designed SHPB dynamic compression test setup.

1.3 Work Summary

In this study, firstly, Al 6061 Aluminum alloy was heat treated by keeping it at 520 °C for 4 hours. Then, samples in 50*40*40 dimensions were prepared. Open die plates were prepared so that the prepared samples could be forged with the multi-axial forging method. The samples were kept at 200 °C for 10 minutes and forged in the x-axis was performed. Afterward, it was cooled in room temperature water and kept at 200 °C for 10 minutes, and forging was performed in the y-axis. It was cooled in the water again and moved to the z-axis. One round beating in x-y-z is called 1 cycle. This process was repeated with a 1-2-3-4 cycle. Then, after the SEM analysis, tensile test, hardness test, and SHPB assembly of the samples were designed and installed, the tests were carried out in this apparatus and the fracture surface between the forging cycles was compared by examining the SEM analysis, microstructure, and mechanical properties.

CHAPTER II

PREVIOUS WORK

2.1 Pure Aluminum and Aluminum Alloys

Natural aluminum, which is soft, nonmagnetic, and easy to shape, makes up around 8% of the earth's crust. Although it is less frequent in the lower layers, It is the most popular metal on Earth and the third most common element in the universe, after silicon and oxygen. It is also the element with the greatest abundance in the soil of the planet. Pure aluminum has never been found in nature, unlike metals like silver and gold. Aluminum alloys play a key role in modern engineering since they are the most used non-ferrous material. They have been widely used in automotive, aerospace, and construction engineering due to their good corrosion resistance, superior mechanical properties along with good machinability, weldability, and relatively low cost [9]. Electrical conductivity is 64.94% IACS (pure Al at 2 °C). Its melting temperature is 660 °C, and its boiling temperature is 2519 °C.

Due to its strong affinity for oxygen, aluminum is hardly found in its elemental form; instead, it is found in oxides or silicates. Feldspars (KAlSi3O8 – NaAlSi3O8 – CaAl2Si2O8), the most common group of minerals in the earth's crust, are aluminosilicates. Aluminum is also found in the minerals beryl (Be3Al2(SiO3)6), cryolite (Na3AlF6), garnet, spinel, and turquoise. Impurities such as chromium and iron in Al2O3 yield gemstone products such as rubies and sapphires, respectively [14].

Even though it is a widely used and prevalent element, not all minerals that contain the element are commercially viable sources of the metal. The resource bauxite

(AlOx(OH)3-2x), which produces almost all metallic aluminum, is used. Bauxite is formed as a decomposition product of low iron and silica bedrock in tropical climates from weathering [15].

There are 7 basic unit cells that are accepted today as simple cubic, triclinic, monoclinic, orthorhombic, rhombohedral, tetragonal, and hexagonal. There are 14 fundamental Bravais cells, in addition to the face-centered cubic (FCC), body-centered cubic (BCC), and hexagonal close-packed (HCP) structures that are ones of these fundamental Bravais cells. Figure 1 illustrates that the structure of aluminum is a face-centered cubic, also known as an FCC.

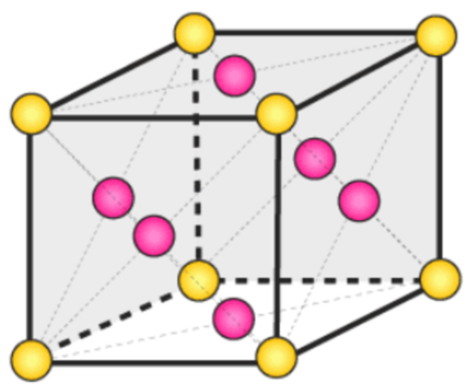

Figure 1: Drawing of Face-Centered Cubic (FCC) unit cell aluminum [16]

The mechanical, physical and chemical properties of aluminum alloys vary depending on the alloying elements and microstructure. The most important alloying elements added to aluminum are copper, manganese, silicon, magnesium, and zinc. Aluminum alloys are divided into two groups as forging and casting alloys. Wrought alloys have good plastic deformation ability and can be easily shaped. Most of the aluminum forging and casting alloys can be heat treated. According to the American aluminum association, aluminum wrought alloys are classified by four letters. The 2xxx, 6xxx, 7xxx, and certain 8xxx alloys are found in forged alloys that make up heat-treatable aluminum compounds [16].

Table 1 shows the different alloying additions and strengthening methods utilized in forged aluminum alloys, along with a brief description of their characteristics and uses [16,17,18].

Table 1: Classification of wrought aluminum alloys [30]

Alloy Series	*Primary Alloying Component* 99%	*Characteristics*
1xxx	99% minimum Aluminum	These series of managed unalloyed aluminum alloys find widespread application in the fabrication of rotors for use in the electrical and chemical industries.
2xxx	Copper (Al-Cu) (Al-Cu-Mg) (Al-Cu-Li)	Copper is the principal alloying element, is generally utilized in the aviation sector because of its 455 MPa yield strength.
3xxx	Manganese (Al-Mn)	Silicon is the most important element in the alloying process. Specifications are provided for the other alloying elements, such as magnesium and copper. The 3xx.x series accounts for close to 90 % of all shaped castings that are manufactured. Alloys with a general purpose are put to use in the building industry, in addition to a great many other items.
4xxx	Silicon (Al-Si)	Silicon is the primary component utilized in the production of alloys, and the 4xxx series can be found in products like welding rods and brazing sheet. The amount of silicon might be anything from 0.6% to 6.2%.
5xxx	Magnesium (Al-Mg)	Magnesium is the primary element that is being used in the alloying process, and the addition range is from 0.2 to 6.2%. Because of their exceptional weldability, 5xxx series products are suitable for a wide range of applications.
6xxx	Magnesium and Silicon (Al-Mg-Si)	Components of 6xxx alloys include magnesium and silicon at a combined 1%. When magnesium and silica are combined, a material that can be solution heat treated to increase its strength is created.
7xxx	Zinc (Al-Zn) (Al-Zn-Mg) (Al-Zn-Mg-Cu)	The main alloying component, with an addition range of 0.8% to 11%, is zinc. Alloys with the 7xxx prefix are the strongest available. The aerospace industry, as well as the aircraft and sports equipment industries, rely heavily on these alloys.
8xxx	Other Elements (Al-Fe) (Al-Fe-Ni)	8xxx is an alloy in which tin is the main component. Add lithium and iron as well.

Table 2: Various strength levels of forged aluminum alloys [30]

Aluminum Association Series	*Type of Alloy Composition*	*Strengthening Method*	*Tensile Strength Range (MPa)*
1xxx	Al	Cold work	70-175
2xxx	Al-Cu-Mg (1-2.5% Cu)	Heat treat	170-310
2xxx	Al-Cu-Mg-Si (3-6% Cu)	Heat treat	380-520
3xxx	Al-Mn-Mg	Cold work	140-280
4xxx	Al-Si	Cold work (some heat treat)	105-350
5xxx	Al-Mg (1-2.5% Mg)	Cold work	140-280
5xxx	Al-Mg-Mn (3-6% Mg)	Cold work	280-380
6xxx	Al-Mg-Si	Heat treat	150-380
7xxx	Al-Zn-Mg	Heat treat	380-520
7xxx	Al-Zn-Mg-Cu	Heat treat	520-620
8xxx	Al-Li-Cu-Mg	Heat treat	280-560

2.2 Al6061 Aluminum Alloy

6061 is a precipitation-hardened aluminum alloy, including magnesium and silicon as its major alloying elements approximately %1. It has good mechanical properties, indicates good weldability, and is mostly extruded. Truck components, railroad materials, pipelines, marine implementation, furniture, agricultural usage, aircraft, architectural implementation, automotive components, building products, chemical equipment, dump bodies, electrical and electronic applications, fasteners, fence wire, fan blades, general sheet metal, highway signs, hospitals, and a multitude of other uses make this one of the most well-known aluminum alloys for general purpose. It is usually existing in pre-tempered grades such as 6061-O (annealed), tempered grades such as 6061-T6 (solutionized and artificially aged), and 6061-T651 (solutionized, stress-relieved stretched and artificially aged). Compositions of Al 6061 alloys and mechanical properties are shown in Table 3-4 [19,20,21,22].

Table 3: Compositions of Al 6061 alloys[30]

Component	*Wt.%*
Al	95.8 - 98.6
Cr	0.04 - 0.35
Cu	0.15 – 0.4
Fe	Max 0.7
Mg	0.8 - 1.2
Mn	Max 0.15
Si	0.4 - 0.8
Ti	Max 0.15
Zn	Max 0.25
Other, each	Max 0.05

Table 4: Mechanical properties of Al 6061 alloys[30]

Ultimate Tensile Strength	310 MPa
Tensile Yield Strength	276 MPa
Elongation at Break	0.12
Modulus of Elasticity	68.9 GPa
Poisson's Ratio	0.33
Fatigue Strength	96.5 MPa
Fracture Toughness	29 MPa-m$^{\frac{1}{2}}$
Shear Strength	207 MPa
Solution Temperature	529 °C
Aging Temperature	177 °C

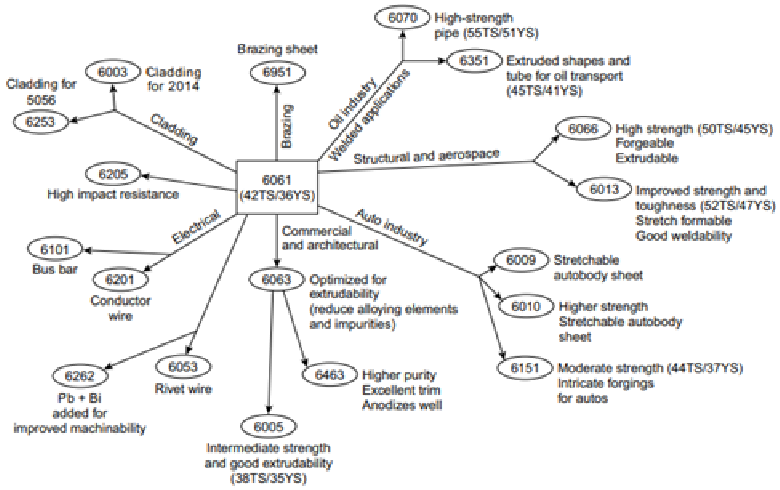

Figure 2: Relationships among commonly used alloys in the 6061 series (Al-Mg-Si). Tensile strength (TS) and yield strength (YS) are in ksi units [30]

2.3 Severe Plastic Deformation (SPD)

One of the most important microstructural variables in polycrystalline light alloys is grain size because of the profound effect it has on the material's chemical, physical, and mechanical properties. The phrase "severe plastic deformation" (SPD) refers to a group of metalworking processes that include very large strains, generally with significant shear or a complicated stress state, leading to large numbers of defects and uniformly sized "ultrafine" grains ($d < 500$ nm) or nanocrystalline (NC) structures ($d < 100$ nm) [23]. According to certain definitions, SPD is a method that applies high strain to a workpiece without significantly altering its dimensions, providing a strong hydrostatic pressure element. However, the mechanisms responsible for grain refinement in SPD are identical to those first developed for mechanical alloying, a powder process described as suffering "severe plastic deformation" by authors as early as 1983 [24].

The majority of SPD research has been on grain refinement, which is obviously relevant to the creation of high-strength materials due to the Hall-Petch connection. Industrial metals that have undergone conventional processing generally contain grains between 10 and 100 μm. When the grain size is reduced from 10 μm to 1 μm, the yield strength of metals can increase by more than 100%. The Hall-Petch equation (1) may be used to observe the direct relationship between grain size and the mechanical, chemical, and physical characteristics of metals [25].

$$\sigma_y = \sigma_0 \ + \ Kd^{-1/2} \tag{1}$$

where k and d are the Hall-Petch coefficient and mean grain diameters, respectively, and σ_0 is friction stress.

For there to be a high density of shear stresses and hydrostatic pressure, there has to be a high density of crystal lattice defects, particularly dislocations, which can considerably refine the grains. This is necessary in order to achieve the high density. In SPD processes, grain refining is accomplished using a multi-step procedure; to lower the overall strain energy, dislocations reorganize and combine together to form ”cells” that are then disseminated throughout the grains, misorientation arises between the cells, creating ”subgrains,” as deformation progresses and additional dislocations are produced, within each subgrain, the process is repeated until the subgrains are tiny enough to spin freely and in the process of further deformation, the subgrains rotate into high-angle grain boundaries, which frequently have an equiaxed structure [26].

Different types of SPD techniques, including constrained groove pressing, cyclic extrusion compression (CEC), repetitive corrugation and straightening (RCS), accumulative roll-bonding (ARB), multi-axial forging (MAF), severe torsion straining (STS), high pressure torsion (HPT), and friction stir processing (FSP), have been developed over the past three decades. The most popular SPD procedures need expensive machinery, including costly dies, high load capacities, a small sample size, and low production efficiencies [16,27,28].

2.3.1 Forging

Forging is a manufacturing technique in which metal is compressed, hammered, or squeezed under intense pressure to create forgings, which are pieces with exceptional strength. The procedure is typically—but not always—performed in a heated setting by preheating the metal to the required temperature before it is worked. Since the metal used to forge products is never melted and poured, forging is a totally different technique than casting (or foundry) (as in the casting process). Stronger pieces may be produced through the forging process than with any other method of metalworking. As a result, forgings are nearly always used in situations where dependability and public safety are critical. However, forgings are rarely seen since they are generally component pieces housed inside completed objects such as airplanes, vehicles, tractors, ships, oil drilling equipment, engines, missiles, and many types of capital equipment, to mention a few [29].

It is possible to forge almost any metal. Aluminum, titanium, brass, copper, and high-temperature alloys including cobalt, nickel, or molybdenum are a few of the most popular metals, as are carbon, alloy, and stainless steels, as well as very hard tool steels. Each metal has various qualities of strength or weight that are best suited to particular pieces, as selected by the customer [29].

2.3.1.1 Forging Machinery

Hammers, Presses, Upsetters, etc. types of equipment can all be used to make forgings, despite the considerable variations in styles and driving systems.

Hammers: Hammers are typically regarded as the most versatile forging tool due to the wide range of forging operations they can carry out. They have been used constantly for both open die and impression die forging. They are distinguished by a large ram that houses the top die. The workpiece is positioned on the bottom die, and the ram is elevated and let to fall or pushed onto it. The bottom or fixed die is held in place and the structure is supported by a large, hefty anvil. High rates of energy application and deformation are produced by hammers. As a result, they perform well with alloys that can bend quickly without producing cracks and breaks in the finished product. This is why most magnesium alloys and aluminum 7xxx alloys are not forged. Hammers are categorized based on how the ram is lifted and whether it falls naturally or is driven. Types of hammers; Board Hammers, Air-lift hammers, Steam or Air-Powered Hammers, Impacters etc. [31,32].

Presses: The second kind of forging equipment that is frequently employed in big open die and impression die forging is forging presses. They are frequently categorized as mechanical or hydraulic depending on how the energy is delivered. Presses generate force more gradually than hammers do. They are utilized for all alloy groups and are preferred over hammers for alloys that need modest deformation rates, such as the majority of magnesium alloys and the 7xxx type of aluminum alloys. They often function vertically, just like hammers. The ram and upper die are joined, and the workpiece feels the power of the ram's downward stroke. Types of presses; Mechanical Presses, Screw Presses, Hydraulic Presses, etc. [31,32].

2.3.1.2 Open Die Forging

Standard flat, "V," concave, or convex dies in presses are used in the hot forming technique known as "open die forging." With this method, components with sizes ranging from a few pounds to over 300 tons may be created. The workpiece is heated to enhance its plastic flow properties and lessen the amount of effort needed to manipulate the metal. While supported by the bottom die, the workpiece is methodically distorted by a succession of blows from the higher die. Advantages of open die process; few or no tooling expenses shorter lead time a range of sizes available, ranging from a few centimeters to almost 100 feet. The disadvantage of open die process; Not appropriate for producing complex, precise pieces or other applications that need tight accuracy, Open-die forgings frequently need to be finished with machining and consistent outcomes, and desirable attributes aren't always produced by processes [31,32].

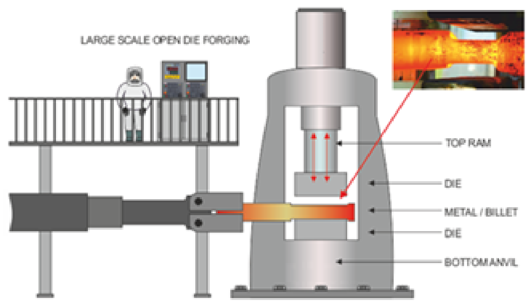

Figure 3: Open die forging processess [31]

2.3.1.3 Close Die Forging

Closed die forgings can be as little as a few ounces or as large as 10,000 pounds, and they can be as long as a few millimeters or as long as 26 feet. The method is largely responsible for all commercial forging output. "Impression die forging" is also known for closed die forging. Though the phrases are occasionally used synonymously, this design guideline distinguishes closed die forging as a unique variety of impression die forging that is covered in more detail below under the topic "flashless forging." Open die forging does not offer the same degree of dimensional control as impression die forging, which gives the workpiece three-dimensional control. A pair of matching dies with custom-made imprints that create an impression or cavity in the shape of the forging are used to create the control [31,32,35]. Advantages of the closed die forging process; better polish on the surface and greater mechanical characteristics, reduced or eliminated machining, cost-efficient for extensive manufacturing runs, it is possible to produce dimensions with more exact tolerances and other forms, more accurate and reliable impressions, the capacity to replicate almost any form or size.

Disadvantages of the closed die forging process; due to the expense of producing dies, short or tiny manufacturing runs are often not financially viable, higher setup costs brought on the expensive equipment and furnaces.

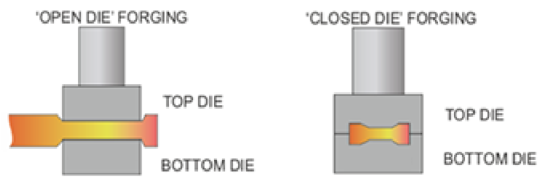

Figure 4: Open and close die forging[31]

2.3.1.4 Hot Forging

The transmission of heat from the metal to the die surfaces results in thermal gradients. Plastic flow is not uniform because it occurs less often on the cooler die surfaces than it does in the hotter core regions. We call this "die cooling." Forging dies for steel forgings are normally heated, depending on the equipment up to an upper limit of 205-260 °C (400-500 °F), in order to reduce cooling. By reducing the contact period, fast-acting forging equipment like hammers, screw presses, and mechanical presses can further minimize the impacts of freezing. The use of glass lubricants is beneficial because they insulate the die and material from heat loss and minimize the die chilling effect. 1700 to 2300°F (925 to 1260°C) is the forging temperature range for steels and titanium and nickel alloys. Specialized tooling materials, such as nickel-based superalloys and molybdenum alloys for dies, and lubricants that can work effectively at these temperatures are required for isothermal forging of high alloys. It's crucial to pay particular attention to the environment, such as by using an inert gas or vacuum to prevent oxidation of the workpiece and the dies.

Both hot die and isothermal forging have pros and cons. The main benefits are tighter forging tolerances, which lowers machining and material costs, a decrease in the number of preforming and blocking processes, which lowers processing and tooling costs, and the use of moderate ram speeds, which uses smaller machines and lower forging pressures. The main cons are the need for more expensive die materials, consistent and precise die heating systems, and an inert environment or vacuum around the dies and workpiece to prevent die oxidation. In order to allow for effective die filling at the low forging pressures, the normal production rates are quite low [33,34].

2.3.1.5 Warm Forging

In order to accomplish warm forging, the workpiece must be heated to a temperature that is typically higher than the work-hardening temperature but lower than the temperature at which scale develops. The technique bridges the gap between the somewhat less precise hot forging technique and the tighter tolerance, but occasionally more expensive cold forging technique. In steel alloys, it is being utilized to make close-tolerance components that cold forging could not or would not be able to create. Additionally, it is being utilized to create components that are manufactured by hot forging and have significant finishing allowances that are extremely similar to the final shape. Currently being warm forged are automobile front-wheel drive shafts and gears [33,34].

2.3.1.6 Cold Forging

One of the most popular chipless forming techniques is cold forging, which frequently requires just drilling as machining. According to the generally recognized definition, forging or shaping a bulk material at room temperature without heating the initial slug or intermediate phases falls under this category. In-process annealing, which may be carried out at interim phases to mitigate the effects of work hardening, is not included in the definition of "no heating." In comparison to hot forming, the procedure yields better dimensional precision and doesn't generate scale. Higher forging pressures are needed since the workpiece's plastic flow properties aren't as excellent. Typically, components can only weigh 50 pounds or less. Cold forgings typically weigh less than 10 pounds [33,34].

Table 5: The main parameters of die forging procedures are compared [33]

Criteria	*Hot forging*	*Warm forging*	*Cold forging*
Forging weight	<60 kg	<10 kg	<2 kg
Shape	Any	Rotational-symmetric	Rotational-symmetric
Roughness	100 µm	50 µm	10 µm
Additional thermal treatment	-	Additional surface treatment is not usually applied	Forcing
Softening pressures	Low	Medium	High
Energy costs	High	Medium	Low
Tolerances	General	Precise	Very precise
Tool costs	Low	High	High
Tool durability (number of items from impression)	5000-10000	10000-20000	20000-50000

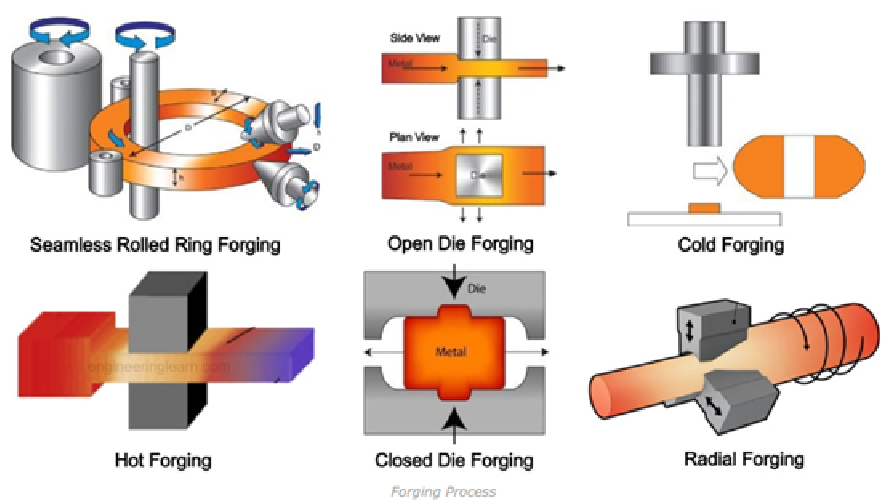

Figure 5: Forging process [34]

2.3.1.7 Multi Axial Forging

The MAF process is a severe plastic deformation method developed in the early 1990s. The most superior feature of this method compared to other SPD methods is that it can be applied to large mass parts at low pressing forces [38,39]. For this reason, the method in question is defined as an SPD method that stands out with its industrial applicability. The method is based on the principle of forging a metal in three main axes one after the other at certain deformation rates. Forging can be done using open and closed dies. The most important disadvantage of this method is known as the inability to provide structural homogeneity and the inability to refine the grain size sufficiently, as in other SPD methods [38,39,40,41]. However, it has been observed that with this method, extremely fine-grained materials can be produced by increasing the number of forging passes and annealing processes [42,43].

In the literature research, it was seen that the grain sizes of metals such as pure aluminum, copper, and titanium were processed with MAF and their mechanical properties were improved. On the other hand, it has been observed that this method has been widely used for the processing of Al-based alloys in recent years [44,45]. As a matter of fact, in this context, it was determined that both the strength and ductility of the 7000 series, 6000 series alloys, and Al-Si-based alloys were increased by multi-directional forging. These outcomes are explained on the basis of grain refinement in alloys, dispersion of hard particles within the structure by fracture, increase in dislocation density, and dynamic recrystallization mechanism [46,47,48]. On the other hand, the number of cycles applied in the MAF process, the total deformation rate, the processing temperature, the structure and mechanical properties of the metals. Found to have a significant effect on its properties. For this reason, it is stated that metals with a steady state can be produced by controlling or selecting the parameters in question. Steady state, on the other hand, is defined as the situation in which the study in grain size is limited, as the dislocation density increases, as the metal reaches sufficient saturation in terms of dislocation. After reaching this state, it was determined that there was no significant change in the structure and properties of metals with increasing the number of cycles [49,50,51].

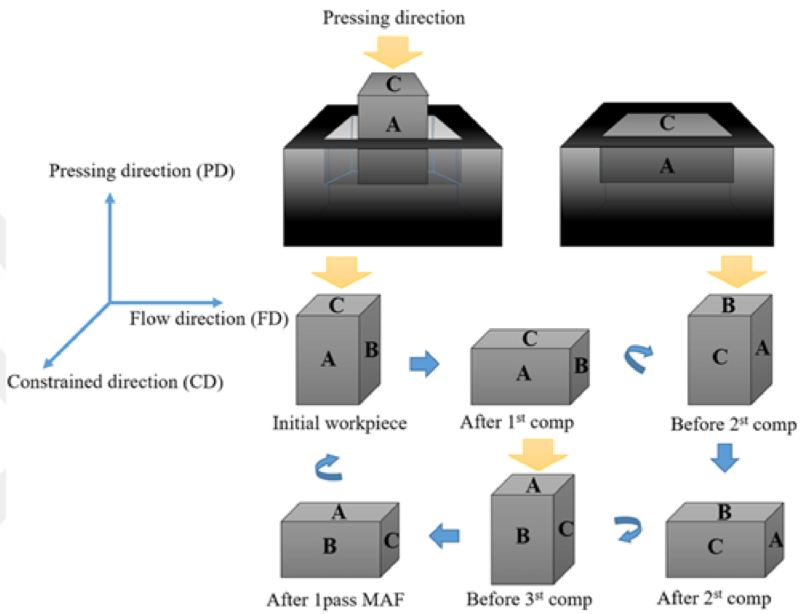

Figure 6: The schematic representation of the applied multi-axial forging (MAF) method [36]

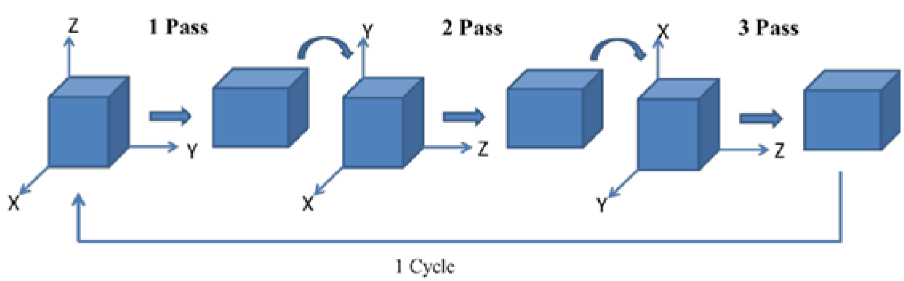

Figure 7: Schematic illustration of Multi axial forging for 1 cycle [37]

2.4 *Dynamic Compression Test (SHPB)*

The split Hopkinson Pressure Bar apparatus and the universal testing machine have both been used in uniaxial compressive studies to determine the dynamic and quasi-static mechanical characteristics of modified double-base propellant at low temperatures [52].

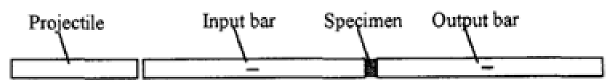

Figure 8: SHPB test set up

$$F_{input}(t) = S_B E \left[\varepsilon_i(t) + \varepsilon_r(t)\right] \quad (2)$$

$$F_{output}(t) = S_B E \varepsilon_t(t) \quad (3)$$

$$V_{input}(t) = C_0 \left[\varepsilon_i(t) - \varepsilon_r(t)\right] \quad (4)$$

$$V_{output}(t) = C_0 \varepsilon_t(t) \quad (5)$$

where ϵ, E and C are respectively, the bar's cross-sectional area, Young's modulus, and the elastic wave speed. A well-liked experimental method for examining the constitutive laws of materials under high strain rates is the Split Hopkinson Pressure Bar (SHPB), often known as Kolsky's apparatus. In 1914 Hopkinson is credited for using a long, thin bar as the first person to do so to measure the pulse shape caused by a hit. After Davies's in 1948 influential work, this approach became widely used. Kolsky developed the experimental design that included two long bars and a short specimen. On a few fundamental presumptions, Kolsky's initial SHPB analysis is built [53]. The theory of one-dimensional wave propagation may be used to describe the waves moving through the bars [54]. The specimen has homogenous stress and strain fields in the axial direction [55]. The impact of specimen inertia is insignificant [56]. The compression test's friction impact is similarly insignificant.

High strain rates of deformation occur in materials in a number of contexts, including engineering applications like vehicle crashworthiness and bulletproof armor and impact resistant pressure vessels and shipping casks for the transportation of nuclear materials, and accidental events like explosions and penetrations. Extrusion, rolling, and high-speed machining are all examples of forming procedures that can result in high-strain-rate deformation. The elements subjected to high strain rates of loading require knowledge of material constitutive behavior at these strain rates for optimal design and risk assessments [57,58].

In order to improve crashworthiness and impact analysis, it is becoming more crucial to test materials dynamically. A potential improvement in energy absorption during a crash event is provided by positive strain rate sensitivity, which is an increase in strength with strain rate. For very high strain rates, the load may be an instant load wave. The machine will also be equipped with the appropriate measuring devices for taking accurate readings of the crucial parameters like strain, displacement, and load [59].

The Split-Hopkinson bar (SHB) operates according to the one-dimensional wave propagation theory. Its primary components are a gas guns, striker bar, incident bar, and transmission bar. The striker bar is housed within the barrel of the gas gun at its chamber. The incident bar, transmission bar, and striking bar are all made from the same materials and have the same cross-sectional area. The test requires the striker, incident, and transmission bars to maintain their elasticity. The sample to be tested is placed in the center of the transmission and incident bars. The striker bar is propelled in the direction of the impact bar by gas pressures [59,60].

When an incident bar and a sample collide, an elastic compression wave propagates along the bar and into the sample. The sample undergoes instantaneous plastic deformation upon arrival due to the repeated wave propagation within it. Both the incident pulse, which travels through the incident bar and out through the transmission bar, and the reflected pulse, which travels back through the incident bar and out via the reflection bar, are detected by strain gauges fitted on the corresponding bars. A strain gauge that measures axial strain is attached to each individual bar. To determine the stress-strain relationship in the sample, an elastic strain created in the incident and transmission bars is used in the calculation [60].

2.5 Effect of Multiaxial Forging on Mechanical Properties of Aluminum Alloys

Material scientists have focused on creating materials with good ductility and strength over the past ten years, but these qualities are frequently incompatible, meaning that a material may have either good ductility or good strength, but not both at once. Microstructure modification must be done in order to improve the properties like ductility and strength [61]. A major progress has been made in severe plastic deformation (SPD) methods. To obtain ultrafine grain structure, several SPD techniques have been developed, including high-pressure torsion, equal channel angular pressing, cyclic closed die forging, multi-axial forging, and many more. Multi-axial forging (MAF) is one of these processes that is most straightforward to execute [62].

To develop a material with tiny grain size, MAF is crucial. MAF is a straightforward process that repeatedly forges the material in three orthogonal dimensions. The sample is rotated 90 degrees after every pass before the subsequent pass is made shown Figure 7. By working at high temperatures, it is utilized to create UFG (ultrafine grain) structure in generally brittle materials. The benefit of MAF is that, even after repeated pressings, the basic form stays the same with little distortion. Additionally, the strain that is applied in MAF is plane strain rather than the simple shear that is produced in ECAP and HPT. As a result, it is probable that the evolution of microstructure during MAF differs from that of ECAP.

Kumar and others in In the current work, UFG Al-Mg-Si alloy was created using the multiaxial forging process at two different temperatures for AlMgSi alloy: (i) ambient 25 °C and (ii) heated 200 °C . Additionally, the treated materials' strength, hardness, J-integral, and plastic strain were examined. To demonstrate a connection between mechanical qualities and metallurgical changes, differential scanning calorimetry (DSC) and electron back scattered diffraction (EBSD) were utilized [63].

Renkó et al. Comparison of multi-axial forging techniques on EN-AW 6082 aluminum alloy using physical and virtual simulation Both physical and digital simulations were created to explore the properties of the EN-AW 6082 aluminum alloy during multiaxial forging. Time, tool motions, temperature, and forces were all recorded during the physical simulation. A finite element simulation was produced using experiment boundary conditions obtained from data. A CAD shape and a typical linear-elastic material model were introduced to the process along with the recorded time, tool motions, and beginning temperature [62].

Yao et al. investigated the effects of multi-directional forging on the extruded 2099 Al-Li alloy's microstructure and properties. After pretreatment and aging, six passes of multidirectional forging were applied to samples of 2099 Al-Li alloy extrusion. According to the findings, multi-directional forging caused the band structure to vanish in the axial direction. Additionally, the grain was refined, having its size decreased from 5004.5 to 2808.6 nm, while simultaneously gaining in tensile strength [64].

Sudheer et al. Multi-axial forging (MAF) was used in the experiment to manufacture light metal aluminum LM6 alloy, which is commercially available. MAF was performed in 0.83, 1.66, and 2.4, or 6 passes, 12 passes, and 18 passes, respectively, to a comparable strain. In both treated and unprocessed samples, mechanical characteristics such as tensile test, compression test, hardness, and microstructural characterization were investigated. From as-received to treated samples, the ultimate tensile strength (UTS) and ductility increased from 137 to 185 MPa and 3 to 6.2%, respectively. The compression strength (CS) increased from 342 to 530 MPa after 18 MAF passes. As the number of forging cycles increased, the hardness increased in contrast to the untreated samples. Microstructure analysis was carried out using microscope images. For the received and treated samples, respectively, the average grain size is decreased from 60 to 2 µm. Due to the grain refinement for the treated samples and the high level of dislocation density introduced into the material during the MAF process, strength and hardness enhanced. SEM was used to perform a fracture investigation, and the ductile mode of fracture was shown by dimples on the surfaces of tension fractures [65].

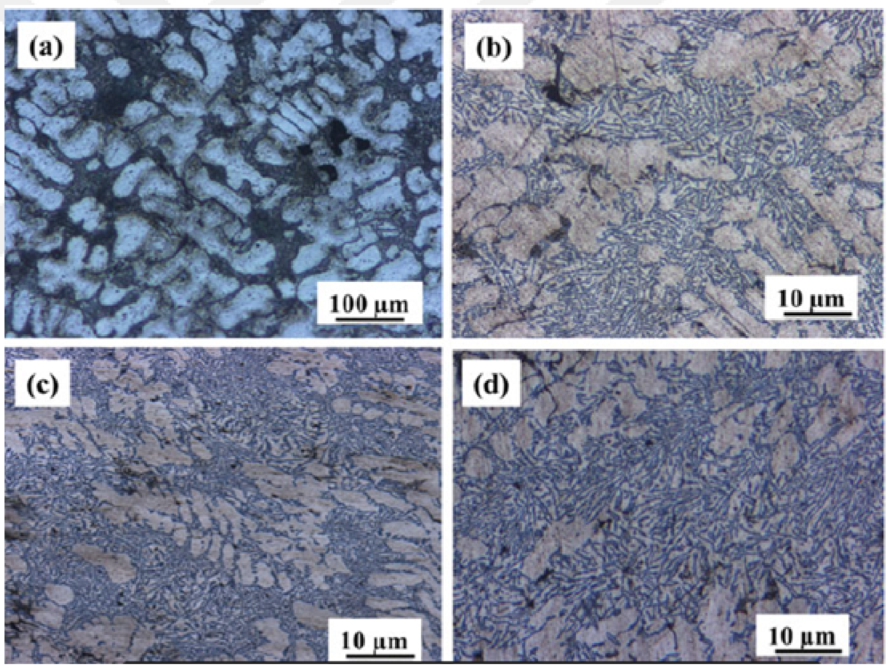

Figure 9: Aspect of silicon particle in the Al–Si specimen a) received sample b) MAF 6 pass c) MAF 12 pass d) MAF 18 pass [65]

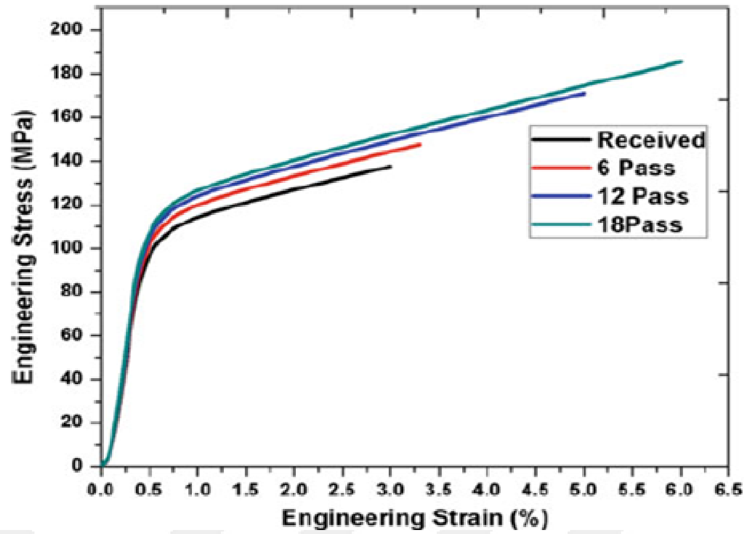

Figure 10: Stress–strain curves for as-received and MAF processed tensile samples [65]

Table 6: Evaluation of grain size and mechanical properties for all the samples processed by MAF [65]

No of MAF passes	*UTS (MPa)*	*CS (MPa)*	*Hardness (VHN)*	*Avg. grain size* (μm)
As-received	137	342	60	±60
6 pass	147	413	72	±15
12 pass	171	486	78	±5
18 pass	185	530	86	±2

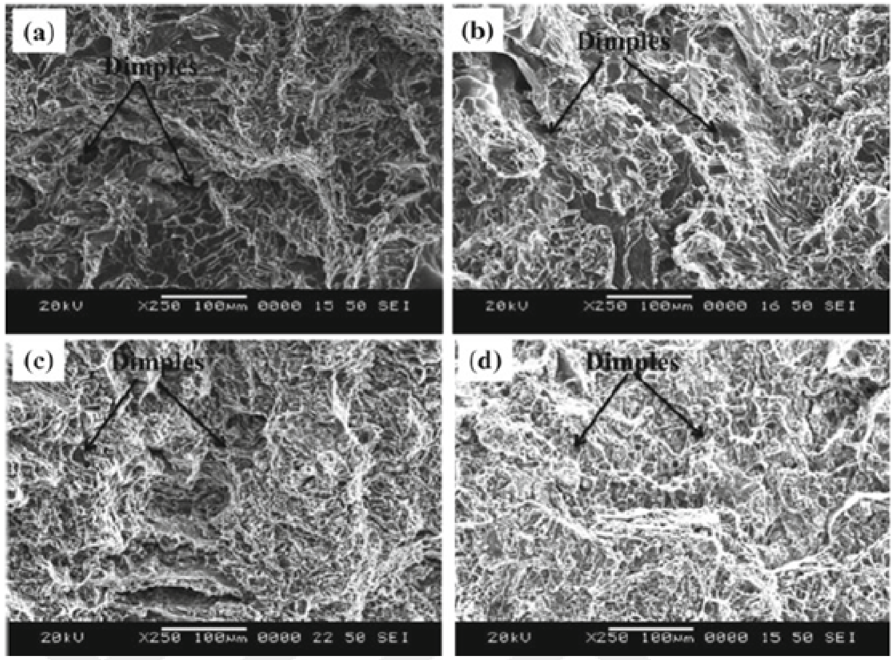

Figure 11: SEM images of tensile fractured of as received and MAF processed a) received b) 6 pass c)12 pass d) 18 pass [65]

2.6 Comparing Quasi-Static Tensile Test and Dynamic SHPB Tests

Kim et al. investigated the Impact of Specimen Thickness on Al6061-T6 Material Property Acquired Using SHPB and Confirmed by FEM. The Split-Hopkinson pressure bar (SHPB), which is utilized to get material characteristics at high strain rates, necessitates careful specimen size selection. As the thickness of the specimen diminishes, the S-S curve increases under the same applied pressure. To understand the impact of specimen thickness on the acquisition of material characteristics, variety of thicknesses specimens of Al6061-T6 material were evaluated under low pressure (1 bar). As a result, the specimen is deformed in the high-strain rate zone, and as the thickness lowers, the S-S curve increases. Furthermore, by doing the test under different pressure circumstances that resulted in similar strain rate areas, the material attributes remained consistent as thickness varied [101]. In the Figure 12-13-14, voltage-time, stress-strain graphs of samples of different thicknesses are compared with the qua-static test results.

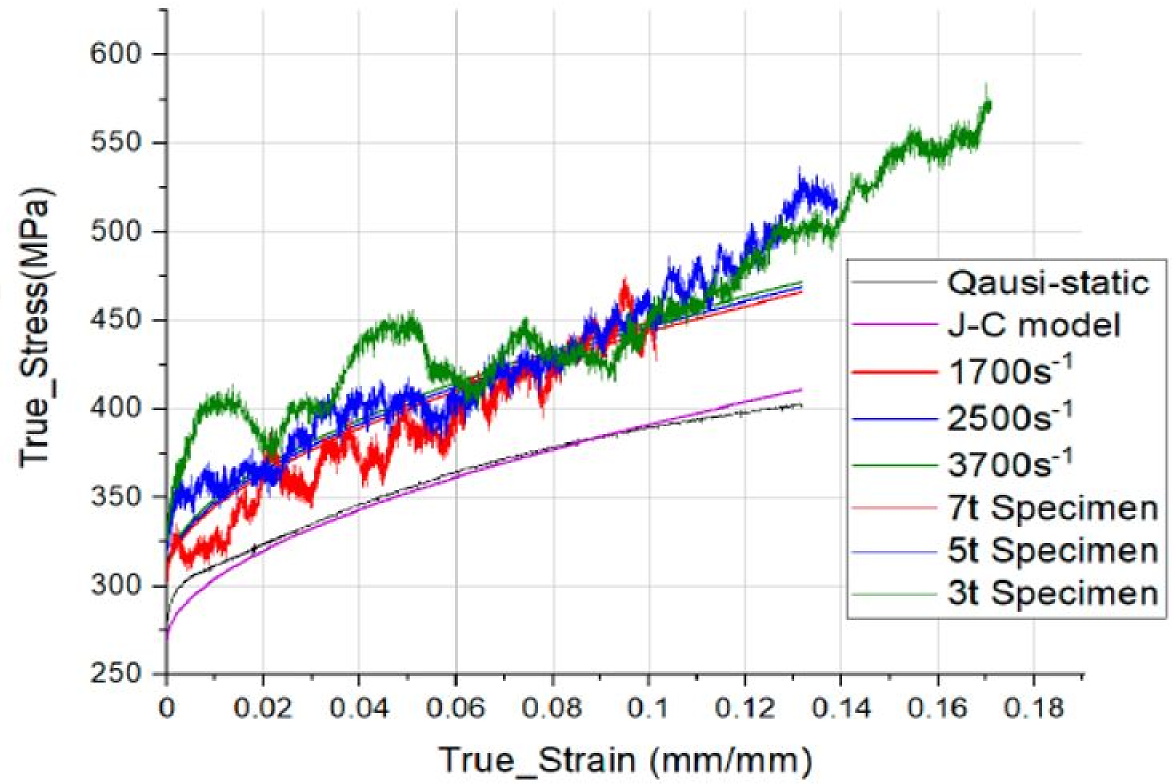

Figure 12: The Al6061-T6 specimen's Johnson-Cook fitting model with the SHPB experimental data [101]

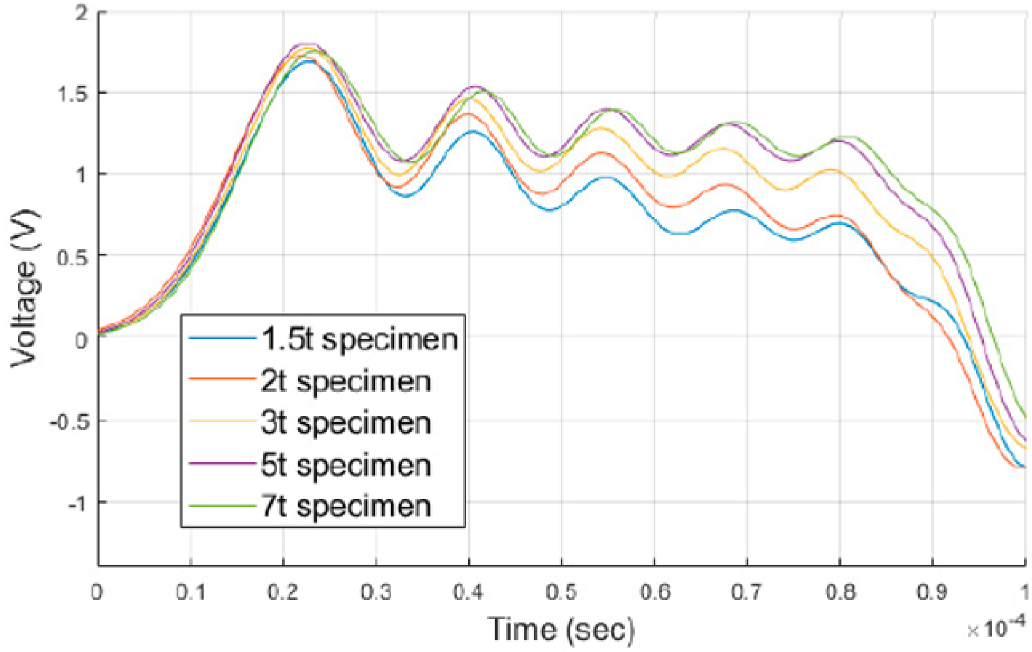

Figure 13: The reflected pulse waveforms were compared for each thickness in the analysis [101]

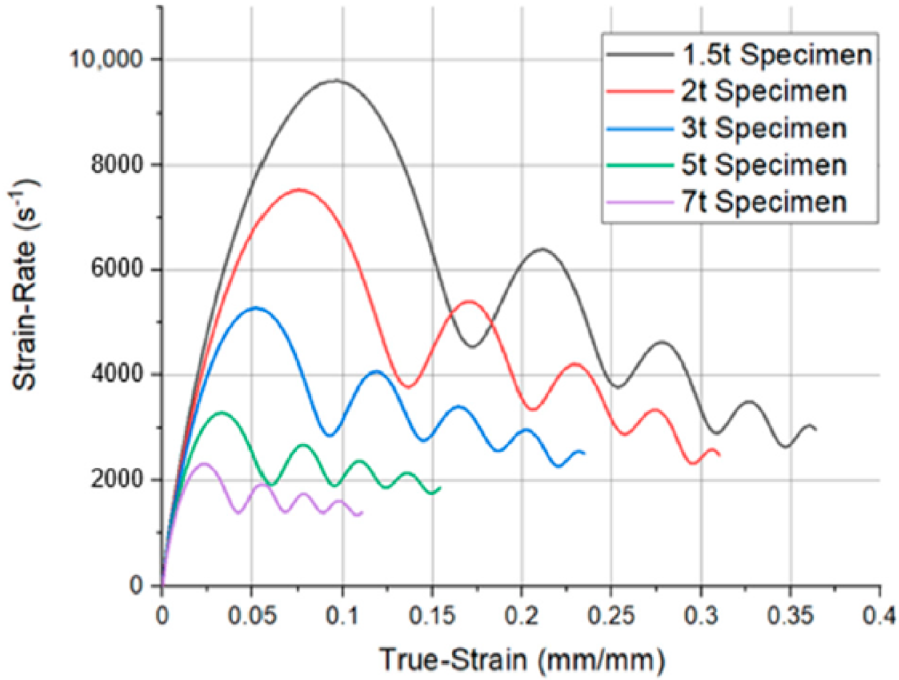

Figure 14: True strain-strain rate graphs were compared for each thickness in the investigation [101]

Mentl et al. researched the drop towers are used for dynamic compression tests, whereas high-speed hydraulic testing equipment or the Hopkinson bar technique used for dynamic tensile tests. Dynamic compression and tensile tests are now feasible thanks to the equipment of a Charpy pendulum testing machine at the Mechanical Testing Laboratory of the Research Inst. in Pilsen, Czech Republic. New striking tups and a load measuring system were developed and fine-tuned. Simultaneously, innovative code was written to analyze the test force-deformation data. Measured and assessed values of energy and deformations were compared to ensure the accuracy of the instruments and software. An excellent compromise was reached [102]. In Figure 14-15, impact test-force results and dynamic and static tensile test results are given comparatively.

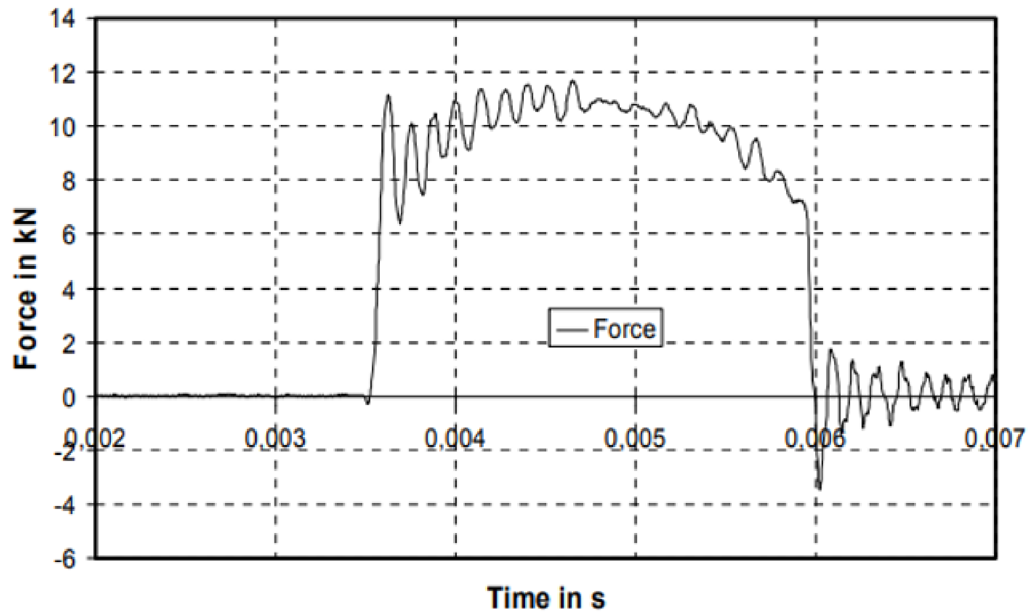

Figure 15: Illustration of a record from an impact tensile test [102]

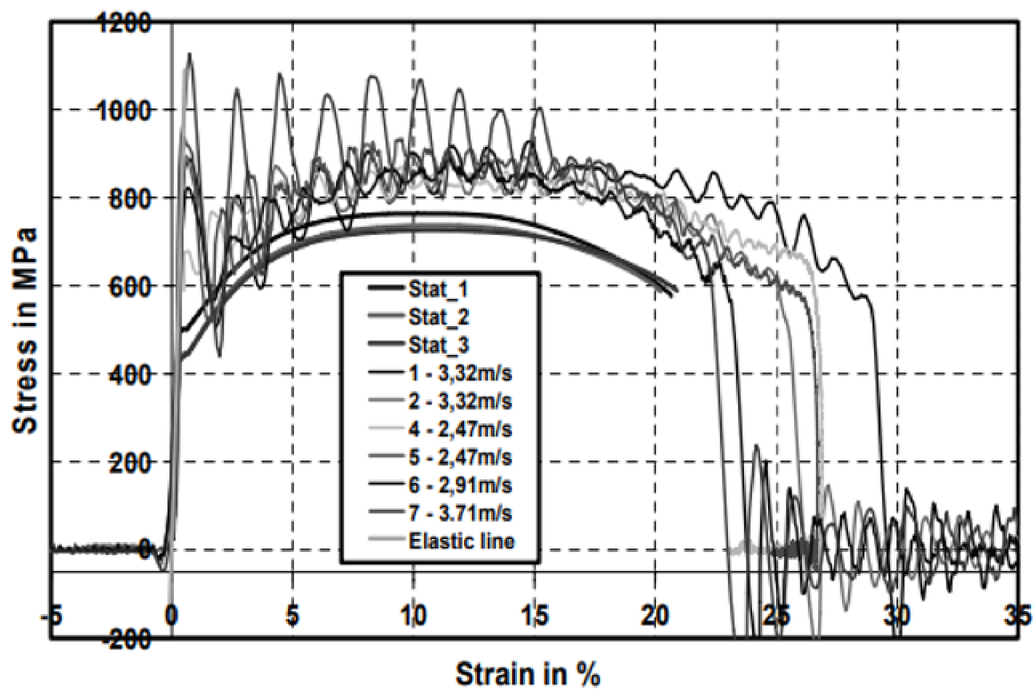

Figure 16: Results of static and dynamic tensile tests are compared [102]

Duan et al. was investigated of the similarities and differences between tensile testing based on the Hopkinson bar for recycled aggregate concrete(RAC). Dynamic direct tensile tests, splitting tests, and spalling tests of recycled aggregate concrete in the varies strain-rate range were conducted using large diameter (75 mm) split Hopkinson tensile bar and pressure bar to compare the tensile properties and fracture patterns of recycled aggregate concrete with different replacement percentages of recycled coarse aggregate. According to the findings of the tests, recycled aggregate concrete has an incredible direct tensile strength, but a less impressive splitting strength when it is in a quasi-static state. The quasi-static tensile strength of recycled aggregate concrete barely varies between a 0% and 75% recycled coarse aggregate replacement percentage. The direct tensile strength and splitting strengths are not the same thing in dynamic tensile testing. In all three types of testing, an increase in average strain-rate enhances the dynamic tensile strength of recycled aggregate concrete [103]. Figure 17 demonstrates that, initially, stress rises linearly. Once yield maximization is achieved, further expansion stops. When the tension is reduced, failure of the specimen begins after it has reached its tensile limit. The peak stress increases as strain-rate rises, demonstrating the influence of RAC on strain-rate.

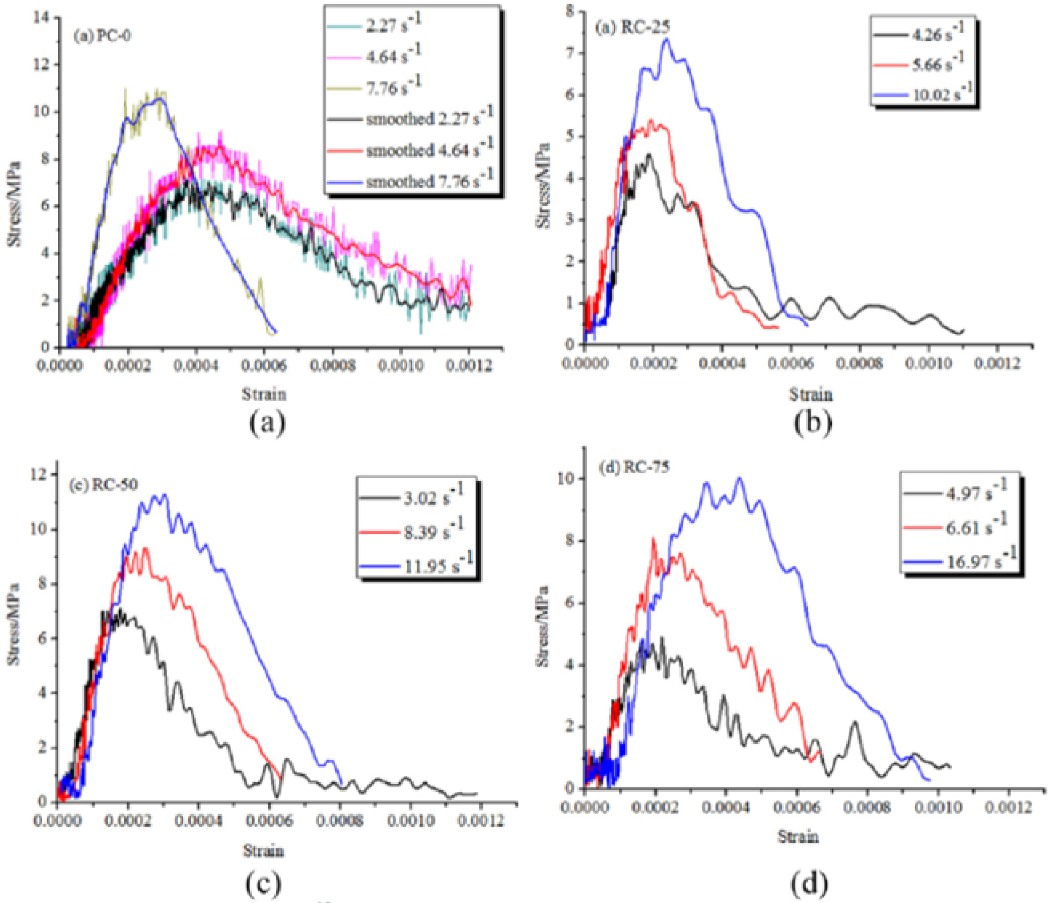

Figure 17: Strain-stress plots of RAC samples: In order: (a) PC-0, (b) RC-25, (c) RC-50, and (d) RC-75 [103]

CHAPTER III

EXPERIMENTAL PROCEDURES

3.1 Material's Characterization and Preparation Processes

In this study, Al -Mg-Si series Al alloy that commercial name Al 6061 was used as as-received material. Below Table 7 gives the as-received Al 6061 slab's chemical composition. The as-received Al 6061 material was cut as the dimensions of 50x40×40 mm with an electrical discharge machining (EDM) process.

Table 7: Chemical composition of Al6061

Element	*Wt.%*
Si	0.63
Fe	0.15
Cu	0.22
Mn	0.03
Mg	0.59
Cr	0.041
Zn	0.009
Ti	0.018
Al	Balance

For the preparation of the as-received materials, a heat treatment is applied to cut Al 6061 slabs at 520°C for 4 hours in the furnace then water is quenched at room temperature. We defined this new sample as ”Base”. This term also mentioned the non-forging sample. Also, the annealing process is needed to restore the formability and homogenize the microstructure of Al 6061 slabs.

3.2 Multi Axial Forging

Samples with dimensions of 50 x 40 x 40 mm were produced by machining from the alloy. The samples were subjected to homogenization before forging. The homogenization process was carried out by keeping the samples in the oven at 520°C for 4 hours and then cooling them in water at room temperature. The forging temperature was determined as 200 °C. After forging analysis, it was decided to forge the samples in an open die. The schematic picture of the forging die and the multi-directional forging process is shown in Figure 18. As seen in the figure, after the sample is forged from its long side in the first pass, it is rotated 90° clockwise and the second pass is passed. Following the completion of the second pass, the sample is turned 90 degrees in the counterclockwise direction, a third pass of forging is carried out, and following this, the cycle forging process that was applied to the sample is finished. Forging was carried out in each pass to create a 30% shortening on the long side of the sample. The true strain value at this deformation rate was calculated as 0.70. After the sample one, two, three, and four cycles and after each pass, the cycles were completed by cooling in water at room temperature, reheating in the oven at 200 °C, and waiting for 10 minutes. Each pass forging was carried out at a press speed of 1 mm/s in a hydraulic press with a capacity of 150 tons. The homogenized states of the samples were defined as Base, and the hot forged states were defined by the expressions MAF 1, MAF 2, MAF 3 and MAF 4.

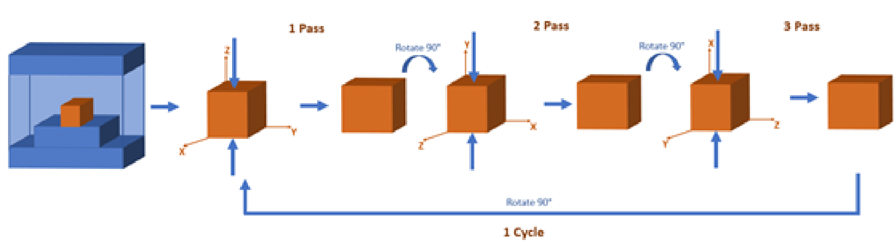

Figure 18: Forging die and one cycle multi-directional forging shown schematically

3.3 Mechanical Behavior Characterization

Figure 19 shows the regions and dimensions of the samples used to analyze the mechanical and structural properties of the Al 6061 alloy obtained by the multi-axial forging method. Tensile test samples (see 3.3.1), 5x5x5 samples were cut and hardness test (see 3.3.2) and SHPB (see 3.3.3) tests were carried out. In order to determine the fracture behavior of the alloy, the vertical sections of the fractured surfaces formed as a result of tensile were examined by the fracture mechanism SEM (see 3.4.2). In addition, grain boundaries and dimensions were examined under the microscope (see 3.4.1).

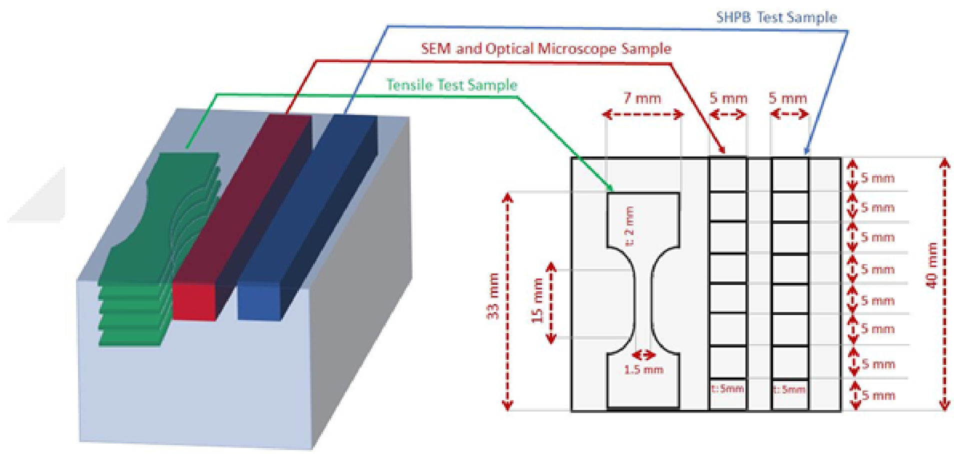

Figure 19: Schematic drawing showing the areas where the samples used in structural and mechanical examinations were taken from the forging and the dimensions of these samples

3.3.1 Tensile Tests

Using electro-discharge machining (EDM), tensile samples were created with a gage length of 15 and a dog-bone form (Figure 19). The samples were ground and polished to get rid of any leftover layers and harmful scratches. An Instron servo-hydraulic mechanical testing frame was put through uniaxial tensile tests with a strain rate of

10^{-3} s^{-1} at ambient temperature.

3.3.2 Hardness Measurement

Testing for hardness is a method for determining a material's hardness that causes the least amount of damage and may be used on a very tiny area. The degree of hardness of a material can give a basic understanding of its behavior by causing the least amount of damage to a sample. Hardness is a quality of a substance, not a basic aspect of physical reality. Its definition is ”resistance to indentation,” and its measurement is ”permanent depth of the indentation.”

ASTM E10 defines the Brinell hardness test technique, which is used to determine Brinell hardness. It is most frequently used to test materials whose structure or surface are too coarse or rough to be evaluated using another test method, such as castings and forgings. A 5 mm diameter ball and a 500 kg load were used for Brinell hardness measurements.

3.3.3 Dynamic Compression Test (SHPB)

The Split Hopkinson Pressure Bar set up used in this study was specially designed and manufactured for the Mechanical Engineering Department of Ozyegin University. The SHPB setup included a launcher with the required gas loading system utilizing the fill valve, an incident bar, a transmitter bar, a striker bar, and a launcher. High-strength steel was used to construct all of the bars. The steel was selected so that even though the specimen received a significant amount of strain throughout the experiment, all of the bars remained elastic. Before the trials began, the sample was carefully wedged between the incident and transmitter bars. SHPB set up schematic diagram seen below Figure 20. The device gives the test results as voltage with the help of strain gauge. Thanks to the special software 'SURE-PulseTM Data Processor', the data received from the system can be read as stress-strain [66].

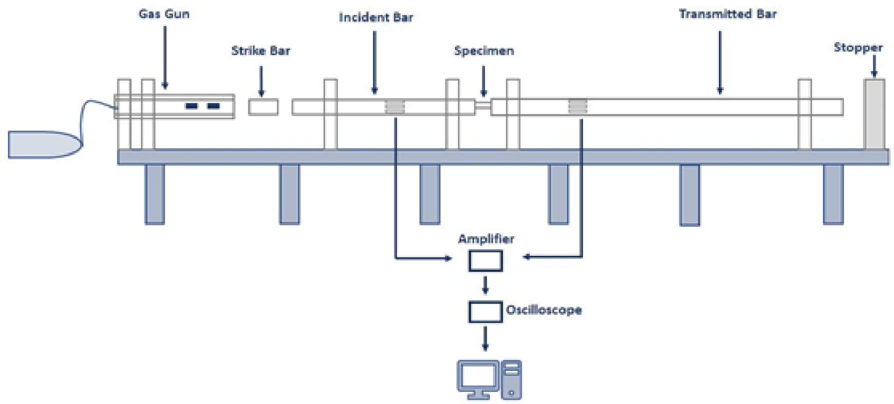

Figure 20: A schematic diagram of SHPB set up

3.4 Microstructural Characterization

3.4.1 Optical Microscopy Observation

After the treatment was finished, samples were chopped with a micro cutting machine into extremely small pieces. After that, samples were mounted using a resin epoxy and hardener mixture for cold mounting.

The standard metallographic preparation method was employed. SiC papers with grit sizes of 400, 600, 800, 1000, and 1200 were used for the grinding process. During the grinding process, water is utilized as a lubricant to prevent the samples' temperatures from rising and the microstructure from being destroyed.

A diamond suspension used 1 µm cloths to mechanically clean the diamonds. To prevent oxidation and surface scratching, an ethanol-based lubricant was utilized throughout the polishing procedure. were washed with ethanol and water following the procedure. Then, etching solution was given for aluminum samples. The Keller's reagent solution, 95 ml water, 2.5 ml nitric acid (HNO3), 1 ml hydrofluoric acid (HF), and 1.5 ml hydrochloric acid (HCl), was used to etch the Al 6061 samples for 20 seconds in order to show grain boundaries. The grains were visible at different magnifications of 10x, 20x, and 50x thanks to a microscope mounted to the camera.

For the microstructure images, it was taken from 3 different sides of the sample as shown in Figure 21 The places shown with x and y are the lateral surface and the number z is the bottom part.

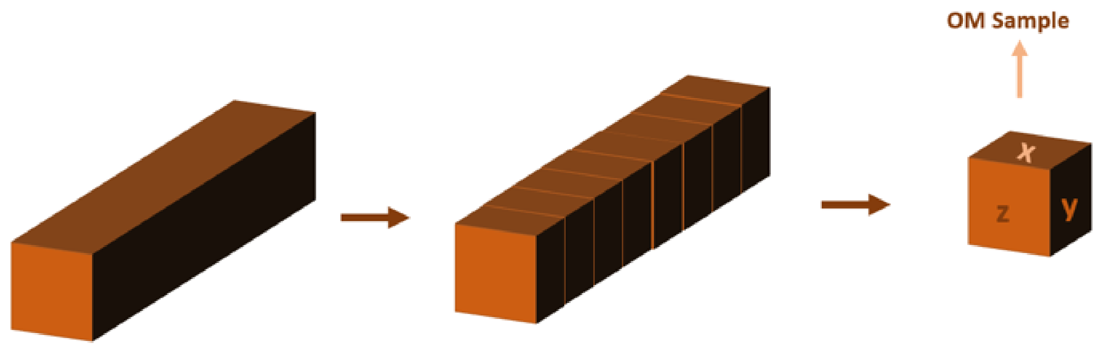

Figure 21: Sampling for microstructure image

3.4.2 Scanning Electron Microscopy (SEM)

A scanning electron beam emits during scanning in scanning electron microscopy (SEM), and an image is created by assembling all signals that are backscattered off the sample's surface. The main electrons projected on the sample's surface are the source of the emitted electrons and other radiation used in image production. Scanning electron microscopy (SEM) was used to examine the fracture morphology under various circumstances for aluminum alloys. This study used jeol JSM-F100 SEM (Figure 22) equipped with an energy-dispersive X-ray spectroscopy (EDS) detector at an accelerating voltage of 20 kV to investigate fracture mechanisms.

Figure 22: Jeol JSM-F100 Scanning Electron Microscope (SEM)

CHAPTER IV

RESULTS AND DISCUSSION

4.1 Microstructure and Hardness Analysis

Optical micrographs of the heat-treated Al 6061 alloy (base sample) are displayed in Figure 23. An average grain length of 13.2 μm is seen in the first microstructure and hardness is 65.5 HB. In Figure 24 shows, the microstructure of the aluminum alloy of MAF1 sample, which has been subjected to 1 cycle multi-axial forging method. As seen in Figure 28, its average grain size is 11.36 μm micrometers and its hardness is 74 HB. When compared with the base sample, it is seen that the hardness increases, and the grain size decreases (Figure 23-24). The average grain size of the 2-cycle MAF sample is 8.32 μm and the hardness is 80 HB (Figure 25). When base-MAF1 and MAF2 samples were compared, it was observed that with the increasing amount of deformation, the grain size in the inner structure of the material became thinner, thus the hardness increased. However, when the microstructure and hardness of MAF3 and MAF4 samples were examined, it was seen that the thesis that the strength of the material increased continuously with the increasing amount of deformation could not be generalized. Material grain size and hardness values of 11.54 μm , 14.46 μm and 73HB, 60HB were obtained, respectively, in 3-cycle and 4-cycle forgings. These values show that the optimum impact value is 6 pass (MAF2 sample) in improving the mechanical properties of Al 6061 alloy by the multiaxial forging method. In the cycles after MAF 2, the grain size increases, and the hardness values decrease (Figure 26-27-28) [67]. Microstructure images were made meaningful by coloring them with image processing. The pyhton programming language was used in the image processing used. The raw microstructure images were given to the program and the image segmentation process was performed. Thus, the grain boundaries became clearer.

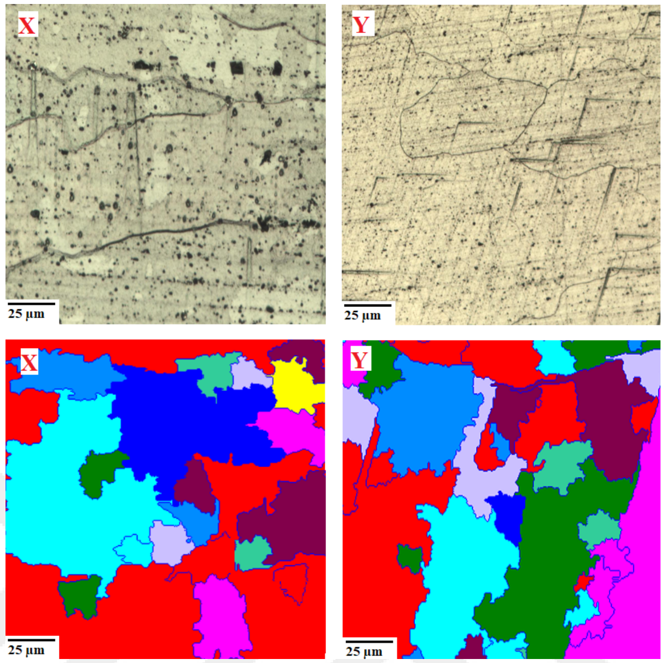

Figure 23: OM Base samples original (top) and image processing (down)

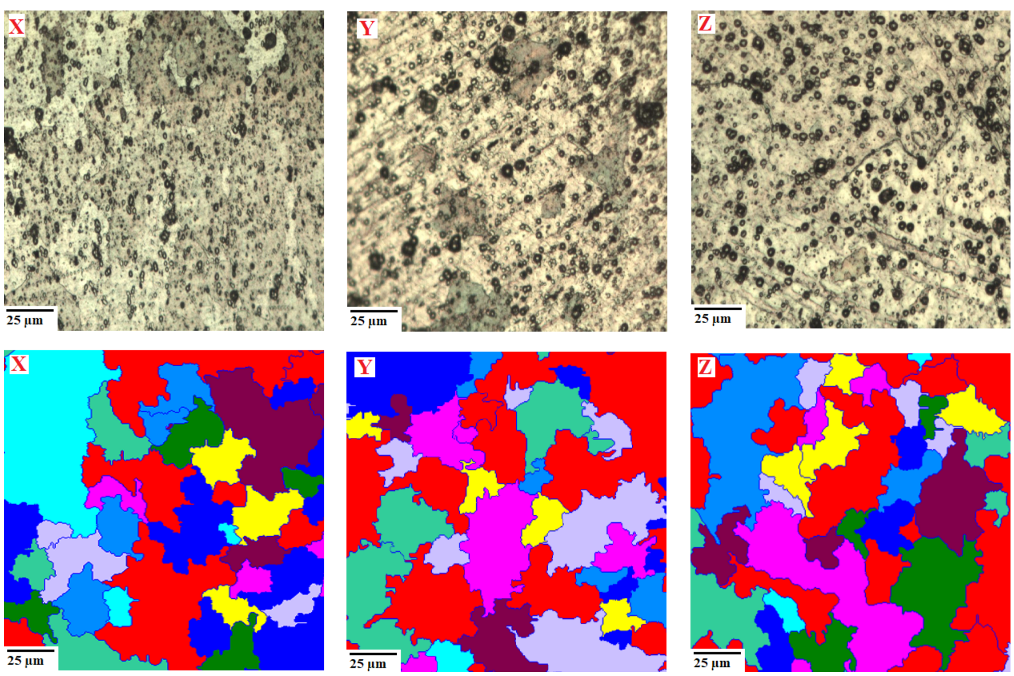

Figure 24: OM MAF-1 samples original (top) and image processing (down)

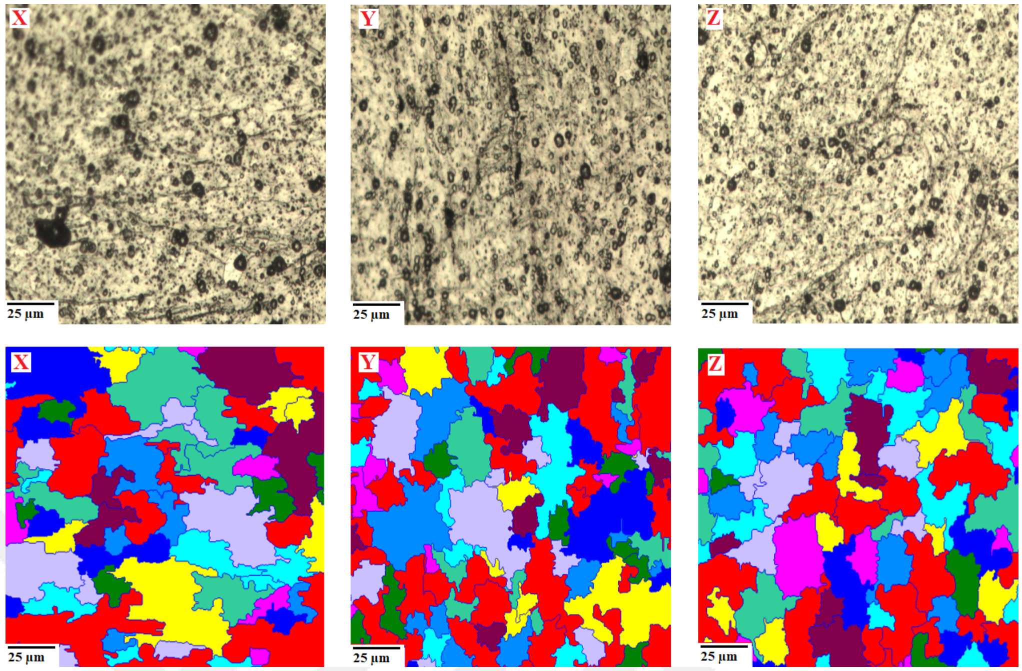

Figure 25: OM MAF-2 samples original (top) and image processing (down)

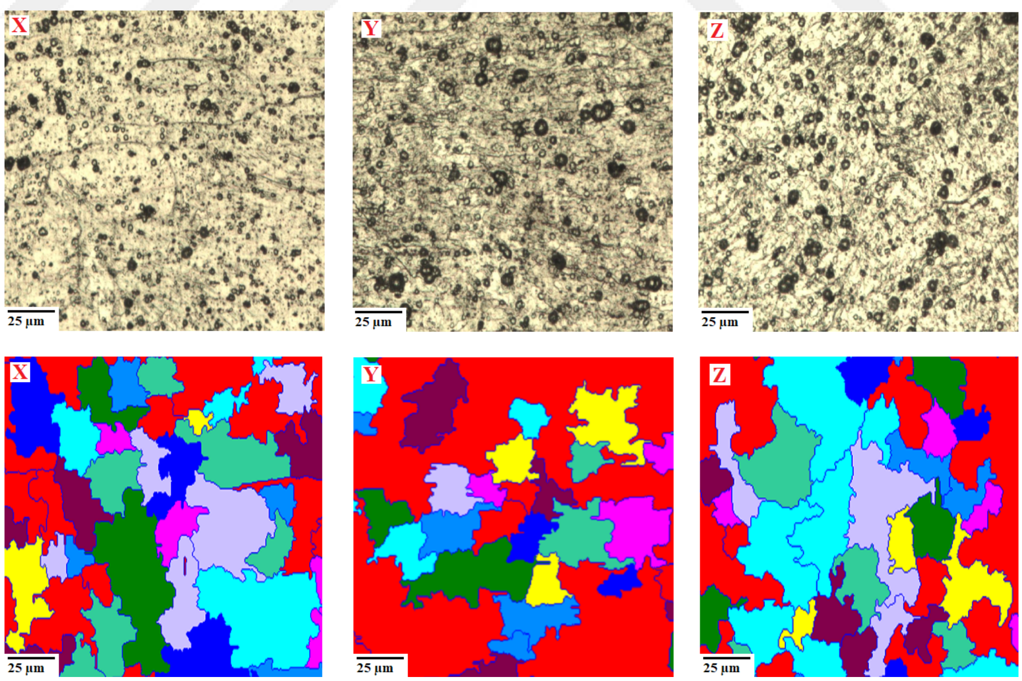

Figure 26: OM MAF-3 samples original (top) and image processing (down)

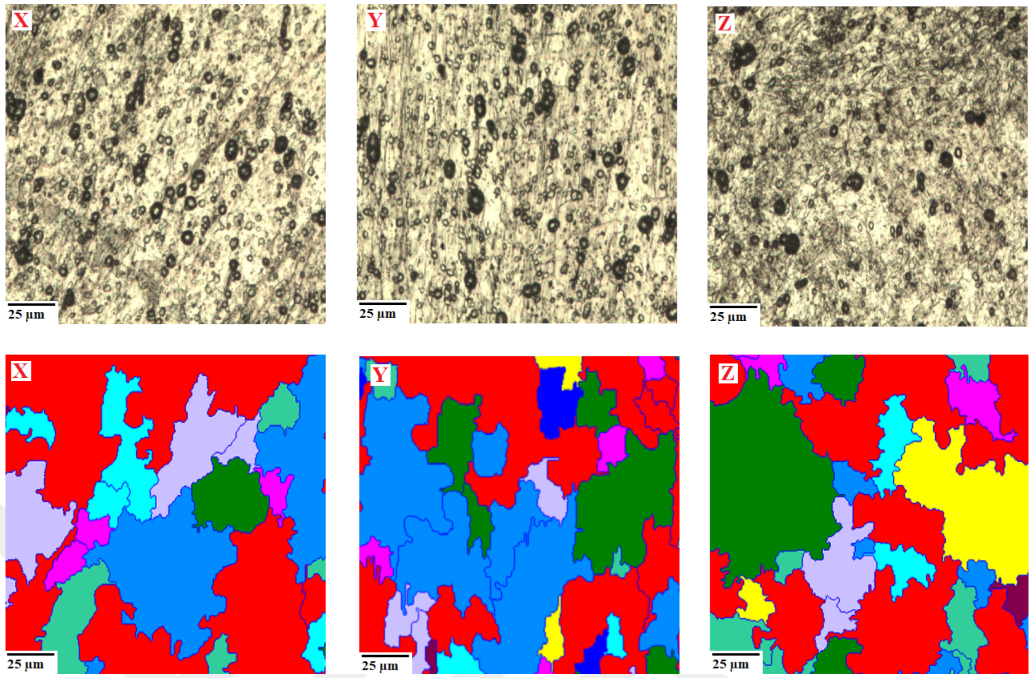

Figure 27: OM MAF-4 samples original (top) and image processing (down)

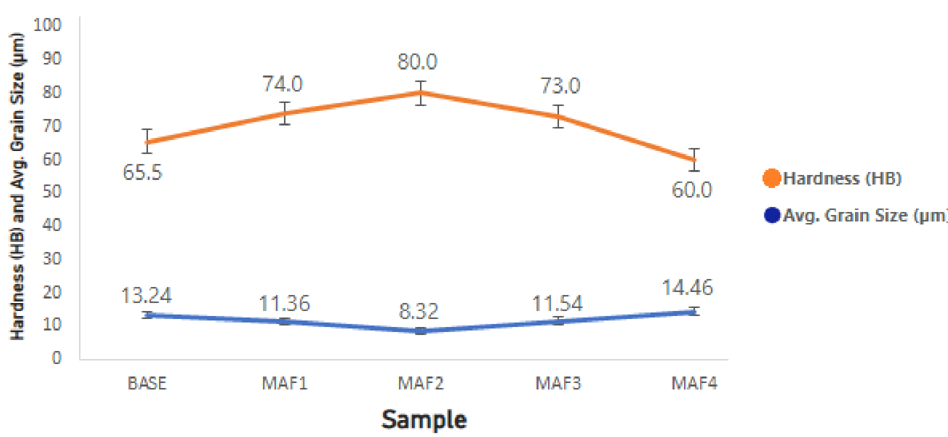

Figure 28: Hardness and Average Grain Size

It has been observed that extremely fine-grained materials can be produced by increasing the number of forging passes and annealing processes with this method [68,69,70]. As a matter of fact, it has been determined that the strengths of the 6000 series alloys and Al-Mg-Si based alloys are increased by multi-directional forging [71,72]. These findings are explained based on grain refinement in alloys, dispersion of hard particles within the structure by breaking, increase in dislocation density, and dynamic recrystallization mechanism. On the other hand, it has been observed that the number of cycles applied in the MAF process, the total deformation rate, and the processing temperature have a significant effect on the structure and mechanical properties of metals.

In addition, it was determined that the strength of this material decreased after 2 cycles (6 pass) of MAF processes. This is explained by the dynamic recrystallization mechanism seen in these materials during the hot forging process [69, 73]. As a result of the multidirectional forging process in the open die applied to 6061 aluminum alloy, it was observed that the number of thinned coaxial grains increased with the change of the deformation axis and the increase in the number of cycles. This situation has been explained by the shear bands formed by the deformation applied from different axes, based on the fragmentation of the grains [74].

Table 8: Average grain size and Hardness test results of Al 6061 base and MAF samples

Sample	*Average Grain Size* μm	*Hardness* (*HB*)
Base	±13.24	65.5
3 Pass	±11.36	74
6 Pass	±8.32	80
9 Pass	±11.54	73
12 Pass	±14.46	60

4.2 Mechanical Properties

4.2.1 Tensile Test

The tensile and hardness test results of Al-Mg-Si (Al 6061) alloy in heat-treated (base) and multidirectional forged conditions are given in Table 9. It was determined that the tensile strength of the alloy in question decreased from 325.36MPa to 228.65 MPa and decreased by approximately 30%, and the yield strength increased by approximately 50% from 132.42 MPa to 197.61 MPa, as a result of a cycle of multidirectional forging. At the end of two cycles, the yield strength reached its highest values. At the end of this cycle, the yield strength was determined as 245.71 MPa, and the tensile strength as 276.9 MPa. These data showed that the two-cycle multi-directional forging process increased the yield strength of the alloy in the heat-treated condition by approximately 85% and decreased the tensile strength by 15%. As a result of 3 and 4 cycles (MAF3 and MAF4), it was determined that the yield and tensile strengths were lower than the results obtained after 2 cycles (MAF2). The values in the 4 cycle (MAF4) results are lower than the 3 cycle results (Figure 29).

On the other hand, when the values obtained as a result of this process were compared with the values of the heat-treated (base) alloy, it was seen that the process increased the yield strength of the alloy by 80% and 44%, respectively, and decreased the tensile strength by approximately 30%. It was determined that the multidirectional forging process increased the hardness of the homogenized alloy and decreased the elongation at break values. While the increase in hardness was 12%, 22% and 12% at the end of 1, 2 and 3 cycles, respectively, at the end of 4 cycles, it decreased by 8% and reached the lowest hardness value.

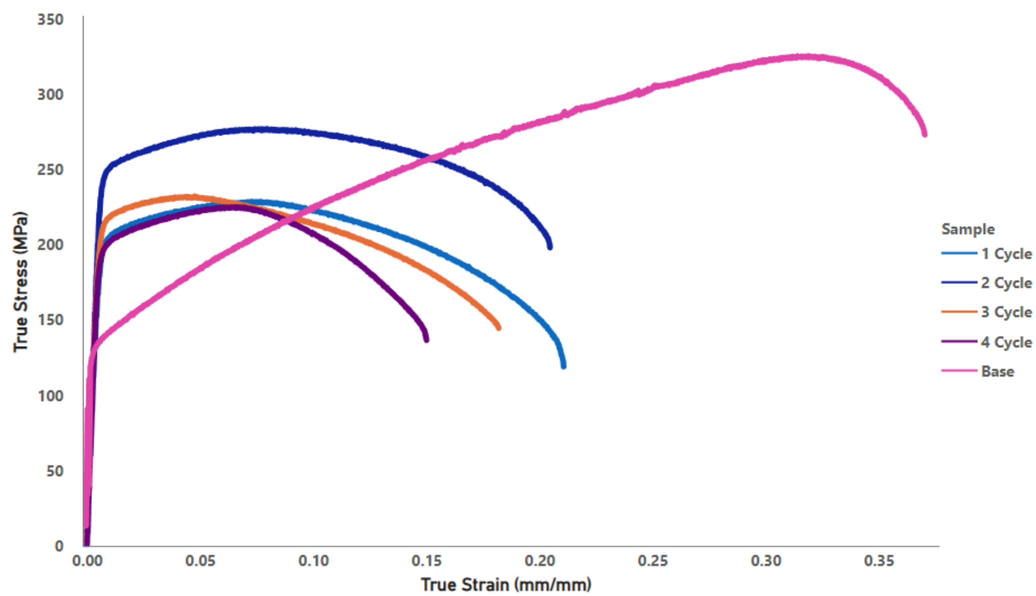

Figure 29: Stress-strain curves for heat-treateed and MAF processed tensile samples

It was determined that the elongation at break value of the heat-treated alloy decreased by 43% after one cycle of multidirectional forging, and by 44%, 51% and 59% after two, three and four cycles, respectively. When these data were examined, it was concluded that increasing the number of cycles in the multidirectional forging process had a significant effect on the yield strength, hardness and elongation at break values rather than the tensile strength of the alloy. These results can be explained based on the morphology and distribution of the silicon particles and the dynamic recrystallization mechanism that occurs in the main matrix (Table 9) [75].

It was determined that the ductility of the alloy decreased, the homogeneous plastic deformation zone narrowed, and the yield strength increased significantly after one cycle forging. In the following cycles, it was observed that the tensile strength of the alloy increased, the homogeneous plastic deformation zone extended, the alloy exhibited a behavior almost independent of strain hardening and its ductility decreased in this region. This behavior of the alloy can be explained by basing it on the structural changes that occur in the alloy. Namely, as the number of cycles increased, it was observed that the hard particles began to break and disperse relatively more regularly into the structure. Shrinkage of hard particles decreases their tendency to form cracks and increases the tensile strength and ductility of the alloy [76, 77, 78, 79, 80, 81]. The sudden increase in the tensile strength and sharp decrease in the ductility of the alloy after one cycle of forging may have resulted from the increase in the dislocation density of the alloy and the inhibition of their movement by the particles involved. However, it is known that recovery, recrystallization, and grain growth occur in the alloy in later cycles with the effect of temperature [82, 83, 84, 85]. These effects lead to the formation of new particles that are relatively free of dislocations in the internal structure of the alloy and decrease the dislocation density [82, 83, 84, 85]. The decrease in the dislocation density causes a decrease in the tensile strength of the alloy [86,87, 88].

When the yield, tensile strength and strength of the alloy were compared with the forged samples, it was determined that the hardness reached its highest values after two cycles of forging and then decreased with the increasing number of cycles. The elongation at the break of the alloy, on the other hand, exhibited the opposite behavior of the properties mentioned above. The fact that the alloy exhibits high mechanical properties and low elongation at break after one cycle of hot forging may be due to the study of hard particles and the increase in the density of dislocations at the end of this cycle [84, 89, 90]. However, the decrease in mechanical properties with increasing cycle numbers is due to the fact that the hard phases break down further and begin to disperse homogeneously into the structure, as well as the decrease in the density of dislocations due to effects such as recovery, recrystallization and grain growth [91, 92]. As a matter of fact, it was observed that the results obtained were in agreement with previous studies on Al-Mg-Si alloys, and it was determined that these changes were explained based on the breaking of hard particles, the decrease in the density of dislocations, and the formation of grains and subgrains [93,94, 95]. The increase in the hardness of the alloys may be due to the dispersion of the silicon particles into the structure as small particles, while the decrease may be due to the dynamic recrystallization of the alloys in the subject [96,97].

Table 9: Mechanical properties of Al 6061 base and MAF samples

Sample	*Yield Stress (MPa)*	*Ultimate Tensile Stress (MPa)*	*Hardness (HB)*	*Average Grain Size* (μm)	*Elongation* (%)
Base	132.42	325.36	65.5	±13.24	37.04
3 Pass	197.61	228.65	74	±11.36	21.07
6 Pass	245.71	276.9	80	±8.32	20.47
9 Pass	212.56	232.34	73	±11.54	18.2
12 Pass	190.89	225.05	60	±14.46	15.01

4.2.2 SHPB Test

The SHPB test is a type of impact test that uses a split Hopkinson pressure bar to generate high strain rates and measure the dynamic behavior of materials. As seen in the figures, the samples were named according to the number of forging cycles they were processed (MAF1-MAF2-MAF3-MAF4). Stress-strain SHPB test results are given in Figure 30, true stress-time SHPB test results are given in Figure 31, True Strain Rate-time SHPB test results are given in Figure 32 and Force-time graphs are given in Figure 33. In these graphs, the behavior of the material in the multi-axial forging process is examined in terms of stress-strain-time and force parameters. When figure 30 is examined, while the strain of the heat-treated sample is 0.016, the stress is 285 MPa, for 3 passes forging (MAF1), while the strain is 0.012 for stress 255 MPa, 6 passes (MAF2), these values are 0.007 - 260 MPa, for 9 passes (MAF3), respectively. the highest stress value was obtained, strain was 0.018 while stress was 310 MPa.

The stress value for 12 passes (MAF4) is 280 MPa, while it is lower than 9 passes but higher than 6 passes. However, the strain value was at the highest value according to all the cycles and was 0.024.

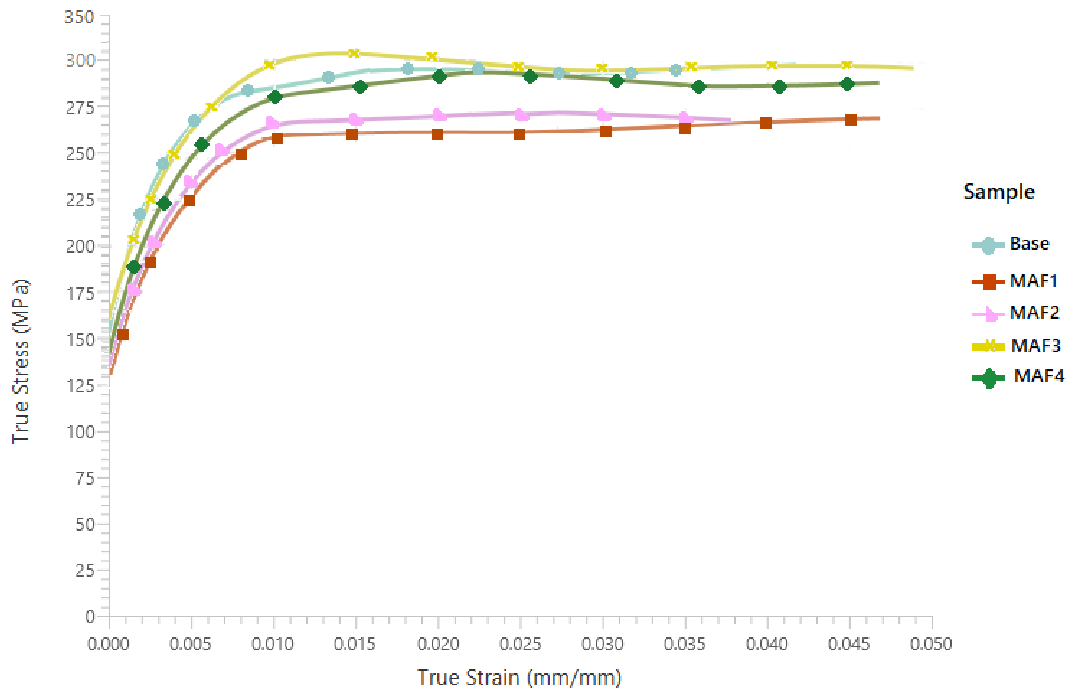

Figure 30: Stress-strain Shpb results

As seen in Figure 31, the test period of the heat-treated material is approximately 8 milliseconds. The test times of the samples, which were subjected to 3-6-9-12 pass forging, are 6, 3.5, 7 and 11 milliseconds, respectively. The MAF4 sample with the longest test time and the shortest time is the MAF2 sample.

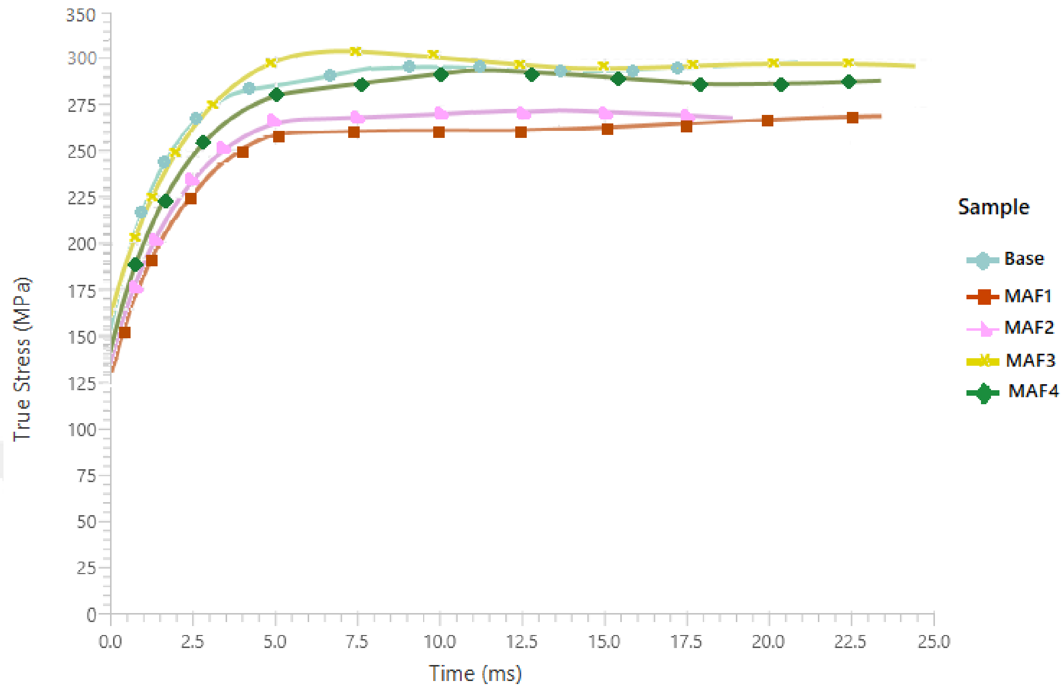

Figure 31: Stress-time Shpb results

The lowest strain rates were observed in the samples where 3 and 6 passes (MAF1 and MAF2) were applied, respectively, and the lowest test times were also observed in these samples. The highest strain rate and stress value were obtained in 9 passes (MAF3) sample Figure 32.

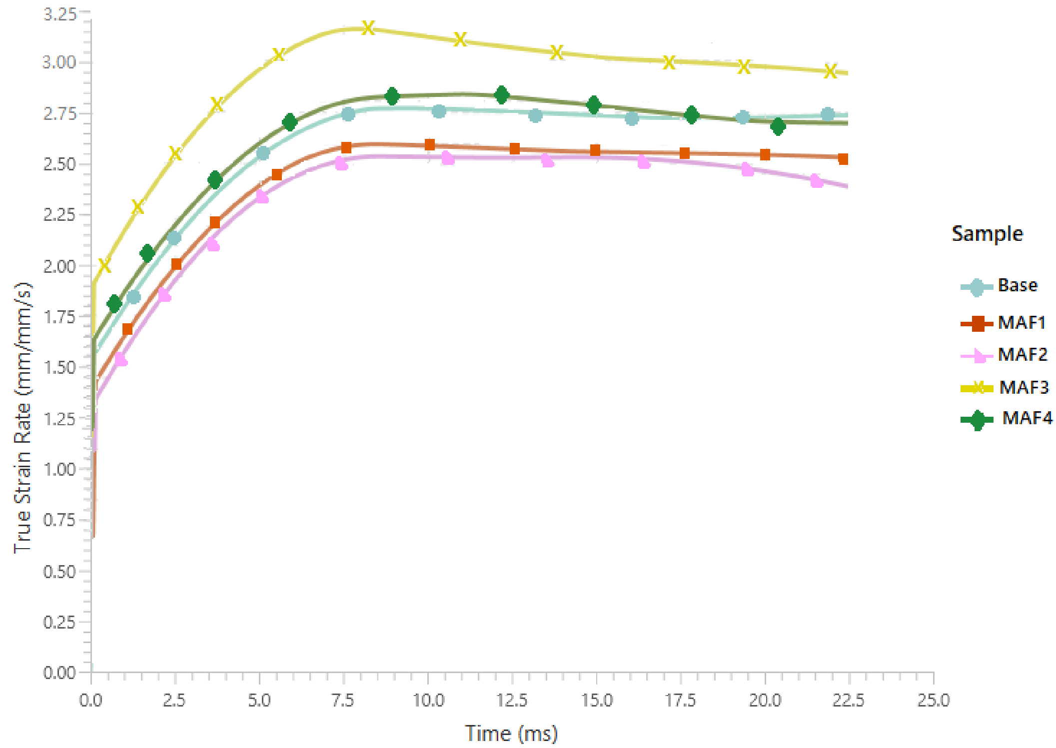

Figure 32: Strain rate-time Shpb results

When we examine the force-time graph in Figure 33, we see that the highest force was obtained as 11000 N in the sample subjected to 9 passes forging. It is seen that the lowest 8500 N value is obtained in the sample subjected to 3 passes (MAF1) forging process. But the back-face forces are lower than these values. For example, while it is 6000N for MAF 3, it is 5000N for MAF1.

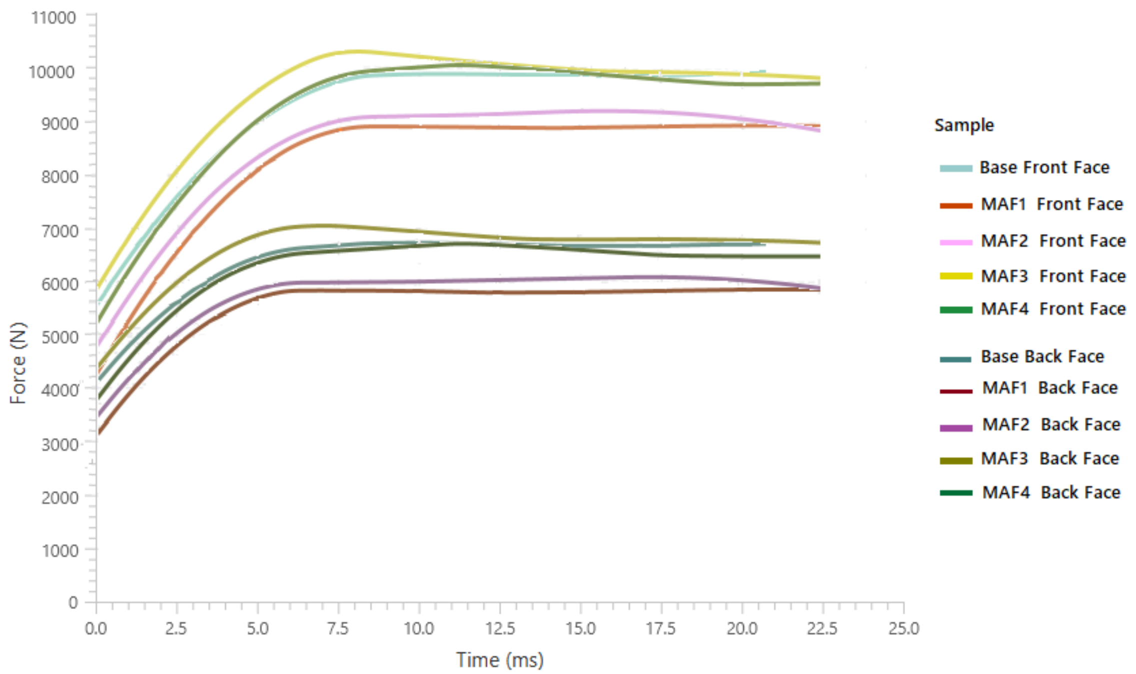

Figure 33: Force-time Shpb results

There is a difference of about 40%. Even when the strain rate is constant, the front and back face forces might vary significantly. It is necessary to assess the tensions at both bar/specimen contacts because of this. In addition to the strain difference between incident and transmitted bars, the amount of energy absorbed due to the material structure should also be considered [98,99].

The stress value is different in quasi-static tensile test and dynamic SHPB test because they have different strain rates and loading modes. A quasi-static tensile test applies a slow and steady load on the material until it breaks, while a dynamic SHPB test applies a sudden and high load on the material that causes shock waves and fracture [106]. The strain rate is the rate of change of strain with respect to time, and it affects the strength, ductility and failure mode of the material. Generally, materials have higher strength and lower ductility at higher strain rates [107]. The loading mode is the way the load is applied on the material, such as tension, compression, shear or bending. Different loading modes cause different stress distributions and deformation patterns in the material. In a quasi-static tensile test, the material is subjected to a uniaxial tension that causes uniform elongation and necking. In a dynamic SHPB test, the material is subjected to a biaxial tension that causes non-uniform deformation and multiple crack [108,109].

4.3 SEM Analysis (Fracture Morphology)

The tensile fracture surface of the alloy Al 6061 under various circumstances is depicted shown in Figure 34. A moderately brittle fracture mechanism is evident on the surface in the form of cleavage facets and steps under all circumstances. The sample that had been heated showed limited ductility with a fracture in tension, and the observations showed that the fracture happened in a brittle way in certain places. Following tensile testing, the fractured surfaces are seen in Figure 34.

The fractured surface of the Al 6061 alloy exposed to MAF at room temperature was examined by SEM in order to comprehend the tensile behavior of the material. The fractured surface of the original condition following heat treatment without MAF is shown in Figure 34a. The fractography reveals a ductile failure pattern with large dimples. The average dimple size has decreased as the MAF cycles have increased, as illustrated in Figure 34b-c. The average dimple size has increased to extremely after 9-12 cycles of MAF, as illustrated in the inset in Figure 34d-e. The smallest grain size, where the measured dimple size almost exactly matches the grain size, was seen after six cycles of MAF2. The quantity of voids that emerge at the grain boundaries and the spot where the fracture first started both affect how big the dimples eventually become [100].

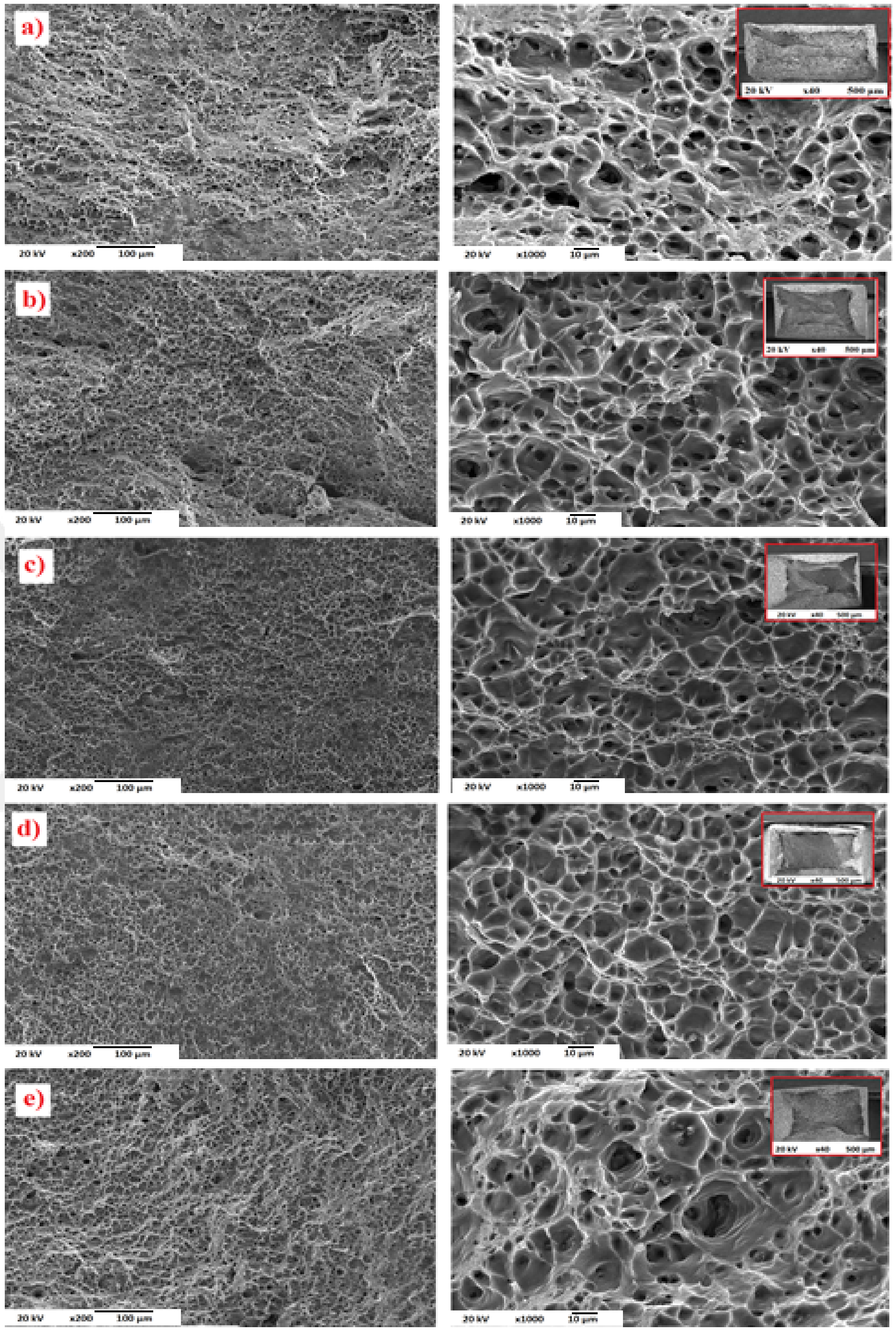

Figure 34: Different processing conditions, and fracture surface of the samples at a)heat-treated(base) b)3 pass (MAF1) c)6 pass(MAF2) d)9 pass(MAF3) e)12 pass (MAF4)

The reason why the yield and tensile strengths increase up to a certain cycle and then decrease in multiaxial forging is the hardening and softening effects that occur during the plastic deformation of the material. Hardening is the increase in strength of the material with deformation. Softening is the decrease in the strength of the material with deformation. The hardening and softening effects depend on factors such as the crystal structure of the material, the deformation temperature, the deformation rate and the amount of deformation.

The hardening effect occurs due to the increase in dislocation density in the material with deformation and the formation of secondary phase particles. Dislocations are line defects that occur in the crystal structure. The greater the dislocation density, the harder the movement of the dislocations and the harder the material. Secondary phase particles are small crystals of different elements in the alloy. Secondary phase particles also inhibit the movement of dislocations and increase the strength of the material. The softening effect occurs due to the reduction of the dislocation density in the material with deformation and the growth or dispersion of the secondary phase particles. As the dislocation density decreases, the movement of the dislocations becomes easier, and the material becomes softer. As the secondary phase particles grow or disperse, they do not obstruct movement of the dislocations and reduce the strength of the material [104,105].

CHAPTER V

CONCLUSIONS

In this study, multidirectional forging process was applied to Al-Mg-Si based Al 6061 alloy containing Silicon and Magnesium, and the effect of the process on the structure and mechanical properties of the alloy was systematically investigated. The results obtained as a result of these investigations are; As the number of cycles increases, the yield and tensile strength of the forged alloy at 200 °C increase. However, this increased amount decreases with the increasing number of cycles after reaching the highest value at the end of two cycles. On the other hand, the ductility of the alloy exhibits the opposite behavior of yield and tensile strength, the multidirectional forging process leads to increased fragmentation of the silicon phase particles in the internal structure of the alloys. As the number of cycles increases, these particles are distributed relatively homogeneously within the structure. This causes the strength to increase, As the number of cycles increases, the elongation at break also decreases continuously.

1- The hardness of forged Al 6061 alloy reaches its highest values at the end of two cycles and these values decrease in subsequent cycles.

2- In the multiaxial forging method, the grain size of the alloy decreases continuously up to two cycles. The lowest grain size is obtained in 2 cycles. (13.24 µm to 8.32 µm) Afer 2 cyles grain size is constantly increasing. (8.32 µm to 14.46 µm)

3- While ductility was observed in the fracture behavior of the heat-treated material, the brittle structure was observed in the samples that processing multi-axial forging.

4- The fractography reveals a ductile failure pattern with bigger dimples. The average dimple size has decreased as MAF cycles have increased.

5- The results of the SHPB test and the results of the quasi-static test show similarity. In both tests, as the number of forging cycles increases up to a certain cycle, the strength values of the sample increase. Likewise, after a certain cycle, the strength values decrease.

CHAPTER VI

FUTURE WORKS

Although certain attempts were made in the current work to explore the microstructure and mechanical behavior of warm multi-axial forged Al 6061 alloy, these techniques are not limited to the tests performed and findings obtained. Consequently, the following recommendations for further research are provided:

1- Testing the same study under different temperatures, the behavior of the material under different temperatures can be examined.

2- The friction and wear properties of the versatile forged alloy can be investigated under different sliding conditions

3- The effect of the multidirectional forging process on the structural properties of the alloy can be examined in detail with TEM, EBSD and XRD, and the effect of the process on the structure can be clearly revealed.

4- After the hot forging process, the effects of the integrated processes consisting of heat treatment and cold forging on the structural, mechanical, and tribological properties of the alloys in question can be examined.

5- Increasing the number of cycles, the formability properties of these materials can be investigated.

6- Mechanical and structural properties of different aluminum series alloys can be studied under different temperatures by the multiaxial forging method.

REFERENCES

[1] Z.-c. Xu, X.-f. Guo, W.-p. Yang, H.-b. Cui, and Y. Wang, "Microstructural evolution and mechanical properties of 6061 aluminum alloy processed with equal channel angular pressing (ecap) and multi-axial compression (mac)," *Materials Transactions*, vol. 60, pp. 2319–2327, 11 2019.

[2] R. Valiev, R. Islamgaliev, and I. Alexandrov, "Bulk nanostructured materials from severe plastic deformation," *Progress in Materials Science*, vol. 45, pp. 103–189, 01 2000.

[3] R. Z. Valiev and T. G. Langdon, "Principles of equal-channel angular pressing as a processing tool for grain refinement," *Progress in Materials Science*, vol. 51, no. 7, pp. 881–981, 2006.

[4] Y. Saito, N. Tsuji, H. Utsunomiya, T. Sakai, and R. Hong, "Ultra-fine grained bulk aluminum produced by accumulative roll-bonding (arb) process," *Scripta Materialia*, vol. 39, no. 9, pp. 1221–1227, 1998.

[5] A. Zhilyaev and T. Langdon, "Using high-pressure torsion for metal processing: Fundamentals and applications," *Progress in Materials Science - PROG MATER SCI*, vol. 53, pp. 893–979, 08 2008.

[6] C. G. de Faria, N. G. Silva Almeida, M. T. Paulino Aguilar, and P. R. Cetlin, "Increasing the work hardening capacity of equal channel angular pressed (ecaped) aluminum through multi-axial compression (mac)," *Materials Letters*, vol. 174, pp. 153–156, 2016.

[7] Y. Jin, H. Baek, S. K. Hwang, Y. Im, and B. Jeon, "Continuous high strength aluminum bolt manufacturing by the spring-loaded ecap system," *Journal of Materials Processing Technology*, vol. 212, p. 848–855, 04 2012.

[8] A. Khan and C. Meredith, "Thermomechanical response of al 6061 with and without equal channel angular pressing (ecap)," *International Journal of Plasticity - Int J Plasticity*, vol. 26, pp. 189–203, 02 2010.

[9] I. Sabirov, M. Murashkin, and R. Valiev, "Nanostructured aluminium alloys produced by severe plastic deformation: New horizons in development," *Materials Science and Engineering A*, vol. 560, pp. 1–24, 01 2013.

[10] R. Valiev, "Nanostructuring of metals by severe plastic deformation for advanced properties," *Nat Mater*, vol. 3, pp. 511–516, Aug. 2004.

[11] A. Knowles, X. Jiang, M. Galano, and F. Audebert, "Microstructure and mechanical properties of 6061 al alloy based composites with sic nanoparticles," *Journal of Alloys and Compounds*, vol. 615, p. S401, 12 2014.

[12] R. Sanders, “Technology innovation in aluminum products,” *JOM*, vol. 53, pp. 21–25, 02 2001.

[13] P. N. Rao, D. Singh, H.-G. Brokmeier, and J. Rengaswamy, “Effect of ageing on tensile behavior of ultrafine grained al 6061 alloy,” *Materials Science and Engineering: A*, vol. 641, pp. 391–401, 08 2015.

[14] A. J. Downs, *Chemistry of aluminium, gallium, indium and thallium*. Springer Science & Business Media, 1993.

[15] “The geology of ore deposits. oxford and new york (w. h. freeman and co.),”

[16] J. Hirsch, B. Skrotzki, and G. Gottstein, “Aluminium alloys : their physical and mechanical properties,” 2008.

[17] J. G. Kaufman and E. Rooy, “Aluminum alloy castings: Properties, processes and applications,” 2004.

[18] J. R. Davis, *Alloying : understanding the basics / edited by J.R. Davis.* Materials Park, OH: ASM International, 2001.

[19] A. Association *et al.*, “International alloy designations and chemical composition limits for wrought aluminum and wrought aluminum alloys (revised 2001),” *The Aluminum Association: Arlington, VA, USA*, 2015.

[20] E. L. Rooy, “Properties and selection: nonferrous alloys and special-purpose materials,” *Metals Handbook*, vol. 2, p. 10, 1990.

[21] S. A. Handbook, “edition, john m.(tim) holt, technical ed; c,” *CINDAS/Purdue University, West Lafayette, IN*, 1996.

[22] A. M. Handbook, “Howard e,” *Boyer and Timothy L. Gall, Eds., American Society for Metals, Materials Park, OH*, 1985.

[23] Q. Wei, S. Cheng, K. Ramesh, and E. Ma, “Effect of nanocrystalline and ultrafine grain sizes on the strain rate sensitivity and activation volume: fcc versus bcc metals,” *Materials Science and Engineering: A*, vol. 381, no. 1-2, pp. 71–79, 2004.

[24] S. Qu, X. An, H. Yang, C. Huang, G. Yang, Q. Zang, Z. Wang, S. Wu, and Z. Zhang, “Microstructural evolution and mechanical properties of cu-al alloys subjected to equal channel angular pressing,” *Acta Materialia*, vol. 57, no. 5, pp. 1586–1601, 2009.

[25] V. Segal, I. Beyerlein, C. Tome, V. Chuvildeev, and V. Kopylov, “Fundamentals and engineering of severe plastic deformation,” 2010.

[26] A. Mishra, B. Kad, F. Gregori, and M. Meyers, “Microstructural evolution in copper subjected to severe plastic deformation: Experiments and analysis,” *Acta Materialia*, vol. 55, no. 1, pp. 13–28, 2007.

[27] T. C. Lowe and R. Z. Valiev, *Investigations and applications of severe plastic deformation*, vol. 80. Springer Science & Business Media, 2000.

[28] T. C. Lowe and R. Z. Valiev, "The use of severe plastic deformation techniques in grain refinement," *Jom*, vol. 56, no. 10, pp. 64–68, 2004.

[29] J. T. Black and R. A. Kohser, *DeGarmo's materials and processes in manufacturing*. John Wiley & Sons, 2017.

[30] J. R. Davis *et al.*, *Aluminum and aluminum alloys*. ASM international, 1993.

[31] L. Çapan, *Dövme Teknolojisi*. TMMOB Türkiye Makine Mühendisleri Odası İstanbul Şubesi, 2004.

[32] L. Çapan, *Metallere Plastik Şekil Verme*. Çağlayan Kitabevi, 2010.

[33] T. Altan, G. Ngaile, and G. Shen, *Cold and hot forging: fundamentals and applications*, vol. 1. ASM international, 2004.

[34] *Soğuk ve Ilık Dövme Semineri : Temeller ve Uygulamalar*, 2004.

[35] Z. Gronostajski, Z. Pater, L. Madej, A. Gontarz, L. Lisiecki, A. Łukaszek-Sołek, J. Łuksza, S. Mróz, Z. Muskalski, W. Muzykiewicz, *et al.*, "Recent development trends in metal forming," *Archives of Civil and Mechanical Engineering*, vol. 19, no. 3, pp. 898–941, 2019.

[36] S. Akbarian, A. Zarei-Hanzaki, H. R. Abedi, R. Unnikrishnan, and R. Moat, "Substructure development and deformation twinning stimulation through regulating the processing path during multi-axial forging of twinning induced plasticity steel," *Advanced Engineering Materials*, vol. 20, no. 11, p. 1800453, 2018.

[37] M. Hussain, P. N. Rao, D. Singh, R. Jayaganthan, and S. Singh, "Comparative study of microstructure and mechanical properties of al 6063 alloy processed by multi axial forging at 77k and cryorolling," *Procedia Engineering*, vol. 75, pp. 129–133, 2014.

[38] Y. Estrin and A. Vinogradov, "Extreme grain refinement by severe plastic deformation: A wealth of challenging science," *Acta Materialia*, vol. 61, no. 3, pp. 782–817, 2013.

[39] I. Sabirov, M. Y. Murashkin, and R. Valiev, "Nanostructured aluminium alloys produced by severe plastic deformation: New horizons in development," *Materials Science and Engineering: A*, vol. 560, pp. 1–24, 2013.

[40] B. Cherukuri, T. S. Nedkova, and R. Srinivasan, "A comparison of the properties of spd-processed aa-6061 by equal-channel angular pressing, multi-axial compressions/forgings and accumulative roll bonding," *Materials Science and Engineering: A*, vol. 410, pp. 394–397, 2005.

[41] G. Purcek, O. Saray, and O. Kul, "Microstructural evolution and mechanical properties of severely deformed al-12si casting alloy by equal-channel angular extrusion," *Metals and Materials International*, vol. 16, no. 1, pp. 145–154, 2010.

[42] Z. Zheng, X. Zhang, L. Xie, L. Huang, and T. Sun, "Changes of microstructures and mechanical properties in commercially pure titanium after different cycles of proposed multi-directional forging," *Metals*, vol. 9, no. 2, p. 175, 2019.

[43] S. Karabıyık, "Çok yönlü dövme İşleminin Çinko ve bakır İçeren al-7si esaslı alaşımların yapı, mekanik ve tribolojik Özelliklerine etkisinin İncelenmesi," Master's thesis, Karadeniz Teknik Üniversitesi, 2019.

[44] Q.-f. Zhu, L. Lei, C.-y. Ban, Z.-h. Zhao, Y.-b. Zuo, and J.-z. Cui, "Structure uniformity and limits of grain refinement of high purity aluminum during multi-directional forging process at room temperature," *Transactions of Nonferrous Metals Society of China*, vol. 24, no. 5, pp. 1301–1306, 2014.

[45] T. Aoba, M. Kobayashi, and H. Miura, "Microstructural evolution and enhanced mechanical properties by multi-directional forging and aging of 6000 series aluminum alloy," *Materials Transactions*, vol. 59, no. 3, pp. 373–379, 2018.

[46] S. Biswas and S. Suwas, "Evolution of sub-micron grain size and weak texture in magnesium alloy mg-3al-0.4 mn by a modified multi-axial forging process," *Scripta Materialia*, vol. 66, no. 2, pp. 89–92, 2012.

[47] S. K. Moghanaki, M. Kazeminezhad, and R. Logé, "Mechanical behavior and texture development of over-aged and solution treated al-cu-mg alloy during multi-directional forging," *Materials Characterization*, vol. 135, pp. 221–227, 2018.

[48] R. Kapoor, A. Sarkar, R. Yogi, S. Shekhawat, I. Samajdar, and J. Chakravartty, "Softening of al during multi-axial forging in a channel die," *Materials Science and Engineering: A*, vol. 560, pp. 404–412, 2013.

[49] T. S. B. Naser, K. Bobor, and G. Krállics, "Tensile behavior of multiple forged 6082 al alloy," *Periodica Polytechnica Mechanical Engineering*, vol. 58, no. 2, pp. 113–117, 2014.

[50] O. Sitdikov, T. Sakai, A. Goloborodko, H. Miura, and R. Kaibyshev, "Effect of pass strain on grain refinement in 7475 al alloy during hot multidirectional forging," *Materials Transactions*, vol. 45, no. 7, pp. 2232–2238, 2004.

[51] P. Sharath, K. R. Udupa, and G. Kumar, "Effect of multi directional forging on the microstructure and mechanical properties of zn-24 wt% al-2 wt% cu alloy," *Transactions of the Indian Institute of Metals*, vol. 70, no. 1, pp. 89–96, 2017.

[52] C. Sun, X. Chen, H. Li, Y. Zhen, and J. Zhang, "Dynamic and quasi-static compressive properties of modified double-base propellant at low temperature," in *Recent Advances in Structural Integrity Analysis-Proceedings of the International Congress (APCF/SIF-2014):(APCFS/SIF 2014)*, p. 417, Woodhead Publishing, 2015.

[53] D. Bancroft, "The velocity of longitudinal waves in cylindrical bars," *Physical Review*, vol. 59, no. 7, p. 588, 1941.

[54] J. Bell, "An experimental diffraction grating study of the quasi-static hypothesis of the split hopkinson bar experiment," *Journal of the Mechanics and Physics of Solids*, vol. 14, no. 6, pp. 309–327, 1966.

[55] L. Bertholf and C. Karnes, "Two-dimensional analysis of the split hopkinson pressure bar system," *Journal of the Mechanics and Physics of Solids*, vol. 23, no. 1, pp. 1–19, 1975.

[56] H. Zhao and G. Gary, "On the use of shpb techniques to determine the dynamic behavior of materials in the range of small strains," *International Journal of Solids and Structures*, vol. 33, no. 23, pp. 3363–3375, 1996.

[57] H. Zhao, G. Gary, and J. R. Klepaczko, "On the use of a viscoelastic split hopkinson pressure bar," *International Journal of Impact Engineering*, vol. 19, no. 4, pp. 319–330, 1997.

[58] J. Shim and D. Mohr, "Using split hopkinson pressure bars to perform large strain compression tests on polyurea at low, intermediate and high strain rates," *International Journal of Impact Engineering*, vol. 36, no. 9, pp. 1116–1127, 2009.

[59] W. Chen, F. Lu, and B. Zhou, "A quartz-crystal-embedded split hopkinson pressure bar for soft materials," *Experimental Mechanics*, vol. 40, no. 1, pp. 1–6, 2000.

[60] H. Zhao and G. Gary, "On the use of shpb techniques to determine the dynamic behavior of materials in the range of small strains," *International Journal of Solids and Structures*, vol. 33, no. 23, pp. 3363–3375, 1996.

[61] S. S. Sajjan, M. V. Kulkarni, S. Ramesh, P. Sharath, V. Kumar, and S. Rajole, "Effect of mechanical properties on multi axially forged lm4 aluminium alloy," *Materials Today: Proceedings*, vol. 24, pp. 1462–1467, 2020.

[62] J. Renkó and G. Krallics, "Comparison of physical and virtual simulation of multi-axial forging processes on en-aw 6082 aluminium alloy," *Materials Today: Proceedings*, vol. 45, 12 2020.

[63] N. Kumar, G. Owolabi, and R. Jayaganthan, "Al 6082 alloy strengthening through low strain multi-axial forging," *Materials Characterization*, vol. 155, p. 109761, 2019.

[64] Y. Wu, X. Xu, Z. Zhang, Y. Zhang, P. Deng, and L. Sun, "Microstructure and property of multi-directional forged 2099 al-li alloy extrusions," *Xiyou Jinshu/Chinese Journal of Rare Metals*, vol. 38, pp. 961–966, 11 2014.

[65] S. S. Sajjan, M. V. Kulkarni, S. Ramesh, P. Sharath, R. Rajesh, and V. Kumar, "Mechanical and microstructural properties of multi-axially forged lm6 aluminium alloy," in *Advances in Manufacturing Technology*, pp. 131–139, Springer, 2019.

[66] R. Inc., "Sure-pulse," 2015.

[67] C. Kobayashi, T. Sakai, A. Belyakov, and H. Miura, "Ultrafine grain development in copper during multidirectional forging at 195 k," *Philosophical Magazine Letters*, vol. 87, no. 10, pp. 751–766, 2007.

[68] B. Cherukuri, T. S. Nedkova, and R. Srinivasan, "A comparison of the properties of spd-processed aa-6061 by equal-channel angular pressing, multi-axial compressions/forgings and accumulative roll bonding," *Materials Science and Engineering: A*, vol. 410, pp. 394–397, 2005.

[69] Q.-f. Zhu, L. Lei, C.-y. Ban, Z.-h. Zhao, Y.-b. Zuo, and J.-z. Cui, "Structure uniformity and limits of grain refinement of high purity aluminum during multidirectional forging process at room temperature," *Transactions of Nonferrous Metals Society of China*, vol. 24, no. 5, pp. 1301–1306, 2014.

[70] W. Liu, M. Chen, and H. Yuan, "Evolution of microstructures in severely deformed aa 3104 aluminum alloy by multiple constrained compression," *Materials Science and Engineering: A*, vol. 528, no. 16-17, pp. 5405–5410, 2011.

[71] M. Rokni, A. Zarei-Hanzaki, A. A. Roostaei, and H. Abedi, "An investigation into the hot deformation characteristics of 7075 aluminum alloy," *Materials & Design*, vol. 32, no. 4, pp. 2339–2344, 2011.

[72] O. Sitdikov, T. Sakai, A. Goloborodko, H. Miura, and R. Kaibyshev, "Effect of pass strain on grain refinement in 7475 al alloy during hot multidirectional forging," *Materials Transactions*, vol. 45, no. 7, pp. 2232–2238, 2004.

[73] R. Kapoor, A. Sarkar, R. Yogi, S. Shekhawat, I. Samajdar, and J. Chakravartty, "Softening of al during multi-axial forging in a channel die," *Materials Science and Engineering: A*, vol. 560, pp. 404–412, 2013.

[74] O. Sitdikov, T. Sakai, A. Goloborodko, H. Miura, and R. Kaibyshev, "Effect of pass strain on grain refinement in 7475 al alloy during hot multidirectional forging," *Materials Transactions*, vol. 45, no. 7, pp. 2232–2238, 2004.

[75] R. Kapoor, A. Sarkar, R. Yogi, S. Shekhawat, I. Samajdar, and J. Chakravartty, "Softening of al during multi-axial forging in a channel die," *Materials Science and Engineering: A*, vol. 560, pp. 404–412, 2013.

[76] C. Cui, A. Schulz, E. Matthaei-Schulz, and H.-W. Zoch, "Characterization of silicon phases in spray-formed and extruded hypereutectic al-si alloys by image analysis," *Journal of Materials Science*, vol. 44, no. 18, pp. 4814–4826, 2009.

[77] Y. Alemdağ and M. Beder, "Dry sliding wear properties of al-7si-4zn-(0-5) cu alloys," *Journal of the Balkan Tribological Association*, vol. 21, pp. 154–165, 2015.

[78] Y. Lee, A. Dahle, D. StJohn, and J. Hutt, "The effect of grain refinement and silicon content on grain formation in hypoeutectic al-si alloys," *Materials Science and Engineering: A*, vol. 259, no. 1, pp. 43–52, 1999.

[79] G. Purcek, O. Saray, and O. Kul, "Microstructural evolution and mechanical properties of severely deformed al-12si casting alloy by equal-channel angular extrusion," *Metals and Materials International*, vol. 16, no. 1, pp. 145–154, 2010.

[80] Y. Alemdağ and T. Savaşkan, "Effects of silicon content on the mechanical properties and lubricated wear behaviour of al-40zn-3cu-(0-5) si alloys," *Tribology Letters*, vol. 29, no. 3, pp. 221–227, 2008.

[81] S. Hegde and K. N. Prabhu, "Modification of eutectic silicon in al-si alloys," *Journal of Materials Science*, vol. 43, no. 9, pp. 3009–3027, 2008.

[82] I. Gutierrez-Urrutia, M. Munoz-Morris, and D. G. Morris, "Contribution of microstructural parameters to strengthening in an ultrafine-grained al-7% si alloy processed by severe deformation," *Acta Materialia*, vol. 55, no. 4, pp. 1319–1330, 2007.

[83] A. Ma, N. Saito, M. Takagi, Y. Nishida, H. Iwata, K. Suzuki, I. Shigematsu, and A. Watazu, "Effect of severe plastic deformation on tensile properties of a cast al-11 mass% si alloy," *Materials Science and Engineering: A*, vol. 395, no. 1-2, pp. 70–76, 2005.

[84] Y. Alemdag, S. Karabiyik, A. V. Mikhaylovskaya, M. S. Kishchik, and G. Purcek, "Effect of multi-directional hot forging process on the microstructure and mechanical properties of al-si based alloy containing high amount of zn and cu," *Materials Science and Engineering: A*, vol. 803, p. 140709, 2021.

[85] C. Liu, B. Qu, Z. Ma, M. Ma, and R. Liu, "Recrystallization, precipitation, and resultant mechanical properties of rolled al-zn alloy after aging," *Materials Science and Engineering: A*, vol. 657, pp. 284–290, 2016.

[86] T. Sakai, A. Belyakov, R. Kaibyshev, H. Miura, and J. J. Jonas, "Dynamic and post-dynamic recrystallization under hot, cold and severe plastic deformation conditions," *Progress in Materials Science*, vol. 60, pp. 130–207, 2014.

[87] E. Galindo-Nava, P. Rivera-Díaz-del Castillo, *et al.*, "Grain size evolution during discontinuous dynamic recrystallization," *Scr. Mater*, vol. 72, no. 73, pp. 1–4, 2014.

[88] S. Gourdet and F. Montheillet, "An experimental study of the recrystallization mechanism during hot deformation of aluminium," *Materials Science and Engineering: A*, vol. 283, no. 1-2, pp. 274–288, 2000.

[89] D. Song, G. Wang, Z. Zhou, E. E. Klu, B. Gao, A. Ma, Y. Wu, J. Sun, J. Jiang, and X. Ma, "Developing a high-strength al-11si alloy with improved ductility by combining ecap and cryorolling," *Materials Science and Engineering: A*, vol. 773, p. 138880, 2020.

[90] M. R. Jandaghi, H. Pouraliakbar, M. K. G. Shiran, G. Khalaj, and M. Shirazi, "On the effect of non-isothermal annealing and multi-directional forging on the microstructural evolutions and correlated mechanical and electrical characteristics of hot-deformed al-mg alloy," *Materials Science and Engineering: A*, vol. 657, pp. 431–440, 2016.

[91] R. Kapoor, A. Sarkar, R. Yogi, S. Shekhawat, I. Samajdar, and J. Chakravartty, "Softening of al during multi-axial forging in a channel die," *Materials Science and Engineering: A*, vol. 560, pp. 404–412, 2013.

[92] M. R. Drury and J. L. Urai, "Deformation-related recrystallization processes," *Tectonophysics*, vol. 172, no. 3-4, pp. 235–253, 1990.

[93] J. Zhao, Y. Deng, J. Tang, and J. Zhang, "Effect introduced high density of precipitates on the microstructural evolutions during multi-direction forging of al-zn-mg-cu alloy," *Materials Science and Engineering: A*, vol. 798, p. 139927, 2020.

[94] M. S. Kishchik, A. V. Mikhaylovskaya, A. D. Kotov, A. O. Mosleh, W. S. AbuShanab, and V. K. Portnoy, "Effect of multidirectional forging on the grain structure and mechanical properties of the al-mg-mn alloy," *Materials*, vol. 11, no. 11, p. 2166, 2018.

[95] J. Wei, S. Jiang, Z. Chen, and C. Liu, "Increasing strength and ductility of a mg-9al alloy by dynamic precipitation assisted grain refinement during multi-directional forging," *Materials Science and Engineering: A*, vol. 780, p. 139192, 2020.

[96] B. Bay and N. Hansen, "Initial stages of recrystallization in aluminum of commercial purity," *Metallurgical Transactions A*, vol. 10, no. 3, pp. 279–288, 1979.

[97] T. Sakai, A. Belyakov, R. Kaibyshev, H. Miura, and J. J. Jonas, "Dynamic and post-dynamic recrystallization under hot, cold and severe plastic deformation conditions," *Progress in Materials Science*, vol. 60, pp. 130–207, 2014.

[98] G. Gray III and W. R. Blumenthal, "Split-hopkinson pressure bar testing of soft materials," *ASM handbook*, vol. 8, pp. 488–496, 2000.

[99] L. Yang and V. Shim, "An analysis of stress uniformity in split hopkinson bar test specimens," *International Journal of Impact Engineering*, vol. 31, no. 2, pp. 129–150, 2005.

[100] Y. G. Ko, D. H. Shin, K.-T. Park, and C. S. Lee, "An analysis of the strain hardening behavior of ultra-fine grain pure titanium," *Scripta Materialia*, vol. 54, no. 10, pp. 1785–1789, 2006.

[101] Y.-B. Kim and J. Kim, "Influence of specimen thickness on the acquisition of al6061-t6 material properties using shpb and verified by fem," *Materials*, vol. 14, p. 205, Jan 2021.

[102] V. Mentl and J. Džugan, "Impact compression and tensile testing by means of a charpy pendulum," *Structures Under Shock and Impact X*, pp. 55–61, 04 2008.

[103] J. Duan, Y. Lu, S. Zhang, and X. Jiang, "Comparative study of tensile tests based on hopkinson bar for recycled aggregate concrete," *International Journal of Protective Structures*, vol. 10, p. 204141961878869, 07 2018.

[104] K. Huang, K. Marthinsen, Q. Zhao, and R. E. Logé, "The double-edge effect of second-phase particles on the recrystallization behaviour and associated mechanical properties of metallic materials," *Progress in Materials Science*, vol. 92, pp. 284–359, 2018.

[105] H. Pang, Y. Liu, J. Luo, C. Li, and H. Li, "Phase/grain boundary assisted-3d static globularization mechanism of tc17 alloy based on the microstructure reconstruction and in-situ tem observation," *Journal of Materials Science Technology*, vol. 157, pp. 246–261, 2023.

[106] J. Wang, L. Ma, F. Zhao, B. Lv, W. Gong, M. He, and P. Liu, "Dynamic strain field for granite specimen under shpb impact tests based on stress wave propagation," *Underground Space*, vol. 7, no. 5, pp. 767–785, 2022.

[107] P. Sreenivasan and S. Ray, "Mechanical testing at high strain rates," in *Encyclopedia of Materials: Science and Technology* (K. J. Buschow, R. W. Cahn, M. C. Flemings, B. Ilschner, E. J. Kramer, S. Mahajan, and P. Veyssière, eds.), pp. 5269–5271, Oxford: Elsevier, 2001.

[108] X. Jin, C. Hou, X. Fan, C. Lu, H. Yang, X. Shu, and Z. Wang, "Quasi-static and dynamic experimental studies on the tensile strength and failure pattern of concrete and mortar discs," *Scientific Reports*, vol. 7, 11 2017.

[109] B. Jiang, M. Atif, Y. Ding, Y. Guo, and Y. Li, "An experimental study on the dynamic flexural tensile behavior of glass," *Engineering Fracture Mechanics*, vol. 266, p. 108417, 2022.

VITA

Burak Bahat received his B.Sc. degree in Metallurgy and Materials Engineering from the Sakarya University, Türkiye, in 2011. He is currently working toward an M.Sc. degree as a research assistant under the supervision of Professor Guney Güven Yapıcı in the Mechanical Engineering department within MEMFIS at Özyeğin University, Istanbul, Türkiye. His main research interests include the mechanical properties of light alloys processed by severe plastic deformation and the design and fabrication of impact-loading test setups.